Do we need alloying elements for Mg implant materials?

N Hort[1], CL Mendis[1], P Maier[2]

[1] *Magnesium Innovation Centre, Helmholtz-Zentrum Geesthacht, Geesthacht, D.*
[2] *University of Applied Sciences Stralsund, Stralsund, D*

INTRODUCTION: Magnesium and its alloys are under discussion for numerous applications as degradable implant materials. Due to the different requirements on implants (geometry, strength, degradation rate, biocompatibility, fatigue behaviour etc.) and their use either in the cardiovascular or musculoskeletal system it is obvious that a property profile can be very broad. To adjust this property profile alloying elements in combination with appropriate processing have to be used. They are the toolbox of the materials scientists to tailor properties according to the implants requirements.

Alloying Elements: Any element besides the matrix element is an alloying element regardless it's amount because in some cases even minor quantities have a measurable effect. In most commercial alloys Be is present in the range of a few ppm (≈ 4 ppm) to reduce the flammability of molten Mg alloys. Other alloying elements influence properties such as castability, strength, corrosion, formability, etc. In commercial alloys the limits of alloying elements are defined and in most case the total amount of impurities has to be below 0.3 wt.-%. Similar limits are not yet set for magnesium implant materials but are a necessity.

Alloy Design: It is important to define a property profile. This means that the properties which are necessary for a certain application need to be identified and also to be quantified. The requirements for an alloy have to come first from the particular requirements of an implant (benchmarks) and secondly from those of the processing. It might happen that an alloy cannot be cast properly or that the formability is limited or not given. In this case either the processing route needs to be changed or the alloy composition has to be adapted in a way that the material can be processed. But the change in the alloy composition may have also an impact on the property profile of the implant alloy and benchmarks may not be reached.

Castability: Casting is usually the first step in any type of production of metallic materials for implants. Alloying elements influence the castability due to the formation of melting/freezing ranges (pure Mg has a melting point of 650 °C), they impact on micro-porosity, viscosity and density of melts, fluidity, hot tearing susceptibility, grain refinement etc.

Strength: Certain strength is required for any implant to fulfil its purpose. To improve the strength of magnesium alloys following strengthening mechanisms are available: cold working (σ_{cw}), grain refinement (σ_{gr}), solid solution strengthening (σ_{sss}), precipitation (σ_{ph}), and dispersion hardening (σ_{dh}, for materials produced by powder metallurgical route). In principle they can be combined additively on the strength of the matrix σ_0 [1,2]:

$$\sigma = \sigma_0 + \sigma_{cw} + \sigma_{gr} + \sigma_{sss} + \sigma_{ph} + \sigma_{dh} \quad (1)$$

From these different strengthening mechanisms only cold working and grain refinement (due to recrystallization) are applicable for pure magnesium but all of them can be applied to alloys. Precipitation and dispersion hardening are in principle comparable but precipitation hardening is in a thermodynamic equilibrium and can be affected by heat treatments when proper alloying elements are selected.

Corrosion: Fe, Cu, Ni, and Co are known to deteriorate the corrosion behaviour when present in the range of more than 100 ppm. Fe, Ni originate often from the primary production of Mg by the Pidgeon process, while Cu originates often from recycling. Co is not a part of any standard Mg alloy and is normally also not present in the processing route.

Formability: Alloying elements are suitable to soften or harden a metallic material or in the case of Mg alloys they can influence texture formation. In general most alloying elements do not influence the hexagonal structure of Mg but only Li is able to do so. At a content of 5 wt.-% the hcp lattice changes to bcc with a better deformability. Additionally it is also known that certain RE additions in minor amounts can weaken the texture.

CONCLUSION: To tailor properties in a broad range alloying elements as well as a suitable processing route are necessary.

REFERENCES: [1] H.E Friedrich, B.L. Mordike (2006), *Magnesium Technology*, Springer-Verlag, Berlin. [2] E. Hornbogen, H. Warlimont, *Metallkunde*, Springer-Verlag, Berlin.

Development of high-strength bioabsorbable Mg alloys suitable for conventional cold-working processes

AJ Griebel[1], JE Schaffer[1]

[1] *Fort Wayne Metals Research Products Corp., Fort Wayne, IN, USA.*

INTRODUCTION: Magnesium and its alloys have attracted considerable attention as a bioabsorbable material for temporary implants, such as endovascular stents or orthopaedic fracture fixation devices [1,2]. Currently available alloys predominantly exhibit the HCP crystal structure, necessitating hot-forming processes. The addition of as little as 6 wt% Li has been shown to induce a cubic structure, dramatically improving the ductility [3]. The benefits of a ductile Mg material would be two-fold: decreased processing costs and cold-work-induced strengthening.

The purpose of this study was to produce and characterize the workability and mechanical strength of four Mg-Li-X alloys for medical applications.

METHODS: Ingots of each alloy (Table 1) were induction melted and extruded at 300°C to a diameter of approximately 4.5 mm. The ingots were then cold-drawn into wires using standard methods and annealed at 350°C. Similar draw-anneal cycles were repeated as necessary until the final anneal at a diameter of 0.9mm. From this diameter, cold work (% reduction of area) curves were established for each alloy. Mechanical performance was evaluated via a tensile test (Instron, Norwood, MA, USA) with a 127mm gage length and crosshead speed of 12.7mm/min.

Table 1. Alloy composition and attained cold work

Alloy	Composition by wt%	Cold Work (%)
1	94Mg-6Li	94
2	89.5Mg-6Li-4Al-0.5RE	75
3	93.75Mg-6Li-0.25Ca	98
4	93Mg-6Li-1Ca	88

RESULTS: The Mg-Li base alloy (alloy 1) exhibited good ductility, achieving 94% cold work. Al and RE additions reduced the attainable cold work, but dramatically improved strength (Figure 1). The addition of 0.25% Ca to the Mg-Li binary improved the formability with a moderate gain in strength. The higher level of Ca resulted in a somewhat brittle, weaker material. Addition of cold work strengthened all materials, most notably in Alloy 2 (Fig 2), reaching a UTS of 495 MPa.

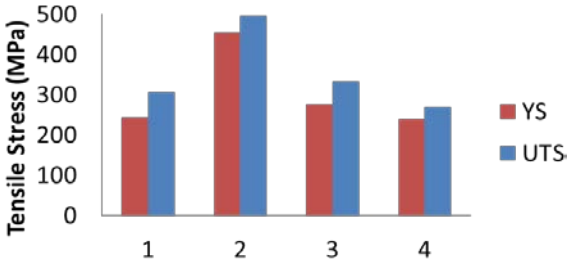

Fig. 1: Yield and ultimate tensile strength values are shown for each alloy at the highest level of cold work attained.

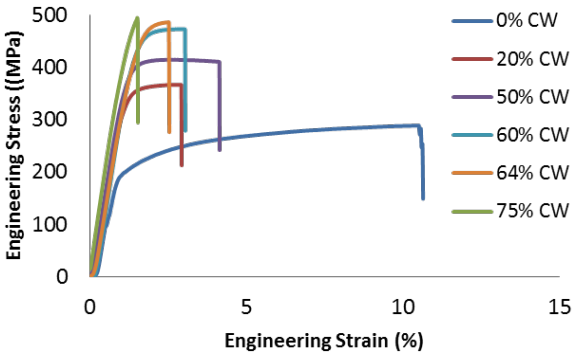

Fig. 2: Tensile curves for Alloy 2 with increasing cold-work.

DISCUSSION & CONCLUSIONS: The need to form currently available magnesium alloys at elevated temperatures is one of the largest contributors to large-scale production cost [4]. The high levels of cold work demonstrated in this study hold promise for a more cost-effective production method.

Excellent strength is an added benefit of cold working. The UTS of Alloy 2 is significantly higher than all conventionally available materials, making it attractive for implant and potential aerospace applications.

Experiments are currently underway to inform the *in vitro* degradation profile of these alloys.

REFERENCES: [1] F. Witte, *et al* (2005) *Biomaterials* **26**:3557-3563. [2] M.P. Staiger, *et al* (2006) *Biomaterials* **27**:1728-1734. [3] M. Sahoo, J.T.N. Atkinson (1982) *J Materials Science* **17**:3564-3574. [4] S. Agnew, (2004) *JOM* May 2004.

Porosity and Young´s-modulus control und measurement on Mg alloy parts, produced by PM (Powder Metallurgy) and MIM (Metal Injection Moulding)

M Wolff[1], T Ebel[1], K U Kainer[1], T Klassen[2]

[1]*Helmholtz-Zentrum Geesthacht* [2]*Helmut Schmidt University, Hamburg*

INTRODUCTION: Recently, the benefits and handicaps of porous Mg-alloy parts for biomedical applications are highly controversial [1-2]. The production of biomedical and biodegradable Mg alloy parts and implants by powder metallurgy (PM) and Metal Injection Moulding (MIM), respectively, offers the opportunity of both, the economic production of porous, as well as nearly dense structures and parts with high complexity in a high number [3]. This study is focussing on methods for porosity and Young´s modulus measurement and control of such parts.

METHODS: Pure Mg powder (SFM-SA, Switerland) and Ca rich master alloy powder (ZfW-Clausthal, Germany) were used for mixing of Mg-0.9Ca powder blends. The PM-route involves the pressing of green compacts at 75 MPa and sintering at 635°C; the MIM-route additionally the adding of polymer binder (PP-co1-PB), injection moulding (Arburg, Germany Allrounder 320S), solvent debinding (Lömi, Germany, 45 °C/10 h) and sintering (Xerion, 635 °C/8-64 h). The time/temperature diagram is shown in figure 1; the detailed process is pointed out in [3-4]. All specimen handling and sintering took place under Ar-atmosphere to prevent powder and parts from picking up additional oxygen.

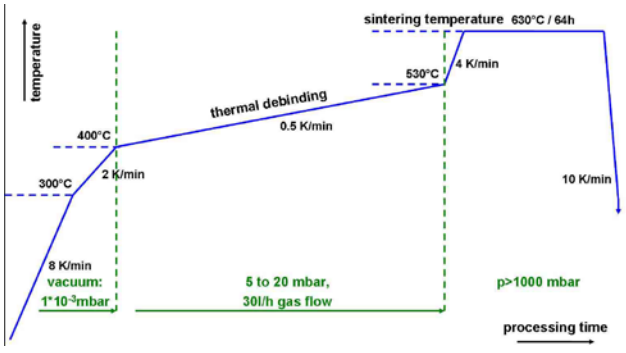

Fig. 1: time/temperature/pressure diagram of the thermal debinding and sintering of Mg-0.9Ca (X1) MIM-parts

The microstructure was studied using light microscopy (Olympus PGM 3) and SEM (Zeiss DSM 962). Additional Photoshop-, analySYS pro software and Archimedes method were used to investigate the porosity. E-moduli were determined by using resonant ultrasonic spectroscopy (RUS), (RFDA, IMCE, Belgium). Materials testing were done by tensile- and compression tests on a Zwick Z005 machine.

RESULTS: The whole MIM processing route, starting from green part production, debinding and in the end consolidation trough sintering, could be successfully performed (see fig. 2).

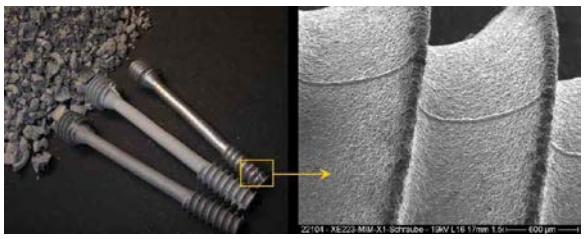

Fig. 2: Green-, debinded- and sintered MIM-part of an implant prototype bone screw made of Mg X1 alloy

In dependence of sintering time, temperature and atmosphere, a residual porosity between 1 % to 8 % and E moduli between 46 to 10 GPa could be achieved. The tensile strength UTS was 131 MPa, TYS was 61 MPa and elongation A_T was 7.7 %. Via compression test a UCS of 242 MPa, UYS of 117 MPa and compressibility A_C of 15 % could be achieved.

DISCUSSION & CONCLUSIONS: The production of controlled porous Mg based implants or implant surfaces, as well as parts with nearly dense areas via Metal Injection Moulding (MIM) seems to be the most advantageous processing route. MIM enables the economic near net shape production of such sophisticated shaped parts in an industrial scale with high degree of automation. In dependence of the particular future medical application, the optimal degree of porosity and interconnectivity has to be evaluated.

REFERENCES: [1] K. Bobe et al. *Acta Biomater.* (2013), 10.1016/j.actbio.2013.03.035. [2] J. Capek, et al *MSE-C* **33** (2013) 564-569. [3] M. Wolff, et al *PIM-International*, Vol.6 No.6 (2012) 59-63 [4] M. Wolff, et al (2010) *AEM* **12**:829-836.

Characterization of biodegradable magnesium single crystals with various crystallographic orientations

KS Shin, HC Jung, MZ Bian, ND Nam, *NJ Kim

Magnesium Technology Innovation Center, Seoul National University, Seoul, Korea
**GIFT, POSTECH, Pohang, Korea*

INTRODUCTION: It is widely known that magnesium alloys are biodegradable in the human body, and could serve better than conventional permanent implants for growth of the new bone. In contrast to traditional permanent implants, therefore, magnesium implants do not need to be removed by a second surgical operation. Due to these advantages, magnesium alloys are the most highlighted materials in recent years for new generation implants [1-3]. In this study, the corrosion behaviour of magnesium single crystals with various crystallographic orientations was examined in order to check the feasibility of magnesium single crystals as new biodegradable implants.

METHODS: Specimens with various desired crystallographic orientations, which are shown in Table 1, were cut from a large single crystal of pure magnesium grown by the modified vertical Bridgman method. The crystallographic orientation of a single crystal specimen for corrosion tests was determined by the Laue back-reflection method. Various corrosion properties were examined using electrochemical techniques such as the potentio-dynamic polarization test, potentiostatic test and electrochemical impedance spectroscopy (EIS) in a 3.5 wt.% NaCl solution.

RESULTS: The potentiodynamic polarization test showed that the specimen with the (0001) surface plane (the 0° specimen) exhibited the highest pitting potential (E_{pit}) among all orientations that were examined. Figure 1 shows results of potentiostatic tests performed at a constant applied potential of -1.57 V_{SCE}. The results showed that the pitting corrosion resistance was highest for the (0001) plane, and subsequently decreased with an increase in the rotation angle from 0^o up to 40^o to 50^o, then increased with a further increase in the rotation angle to 90^o (the (10-10) plane).

DISCUSSION & CONCLUSIONS: The potentiodynamic and potentiostatic results with various crystallographic orientations show that the (0001) and (10-10) planes have higher pitting resistance than other crystallographic orientations. The results indicated that the incorporation of passive film on the specimen surfaces of the low-index planes (the (0001) and (10-10) planes) was facilitated and could enhance corrosion resistance.

Table 1. Crystallographic orientations of the specimens.

Rotation Angle from [0001] to [10$\bar{1}$0] (Degree)	Surface Plane
0°	(0 0 0 1)
10°	(191 0 $\bar{1}\bar{9}\bar{1}$ 2031)
20°	(376 0 $\bar{3}\bar{7}\bar{6}$ 1938)
30°	(549 0 $\bar{5}\bar{4}\bar{9}$ 1785)
40°	(706 0 $\bar{7}\bar{0}\bar{6}$ 1579)
50°	(842 0 $\bar{8}\bar{4}\bar{2}$ 1326)
60°	(952 0 $\bar{9}\bar{5}\bar{2}$ 1030)
70°	(1032 0 $\bar{1}\bar{0}\bar{3}\bar{2}$ 705)
80°	(1083 0 $\bar{1}\bar{0}\bar{8}\bar{3}$ 359)
90°	(1 0 $\bar{1}$ 0)

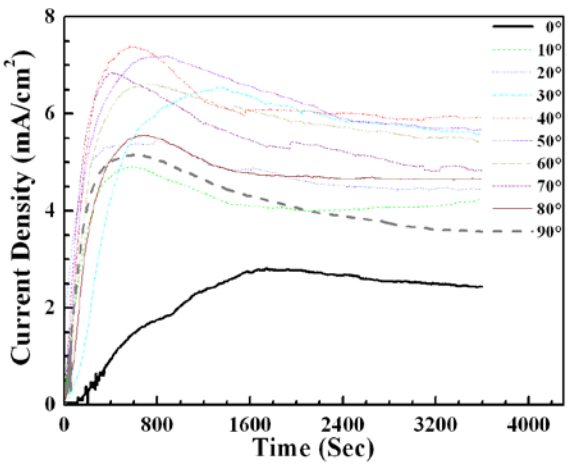

Fig. 1: Change in the current as a function of time with an applied potential of -1.57 V_{SCE}.

REFERENCES: [1] J.H. Jo et al. (2011) *J Mater Sci: Mater Med* **22**:2437-2447. [2] H.S. Han et al. (2012) *Met Mater Int* **18**:243-247. [3] K.S. Shin, M.Z. Bian, N.D. Nam (2012) *JOM* **64**:664-670.

ACKNOWLEDGEMENTS: This work was financially supported by the WPM Program, funded by the Korean Ministry of Trade, Industry and Energy through the Research Institute of Advanced Materials.

Preparation, mechanical and degradation properties of Mg-based microwire for self-assembly stents

Q Peng[1], H Fu[1], J Zhang[2], Y Tian[1], R Liu[1]

[1]State Key Laboratory of Metastable Materials Science and Technology, Yanshan University, Qinhuangdao, 066004, China. [2]Key Laboratory of Superlight Materials & Surface Technology, Harbin Engineering University, Harbin 150001, China.

INTRODUCTION: The implantation of degradable Mg-based stents probably achieves the ideal restoration process of arterial vessel, in which the implantation provides suitable mechanical support within a reasonable period for remodeling the artery in combination of the elimination of both subacute stent thrombosis and in-stent re-stenosis [1]. However, the conventional method is not appropriate to prepare homogenous Mg stents. In this work, a modified extraction method is introduced to prepare Mg microwires directly. Hereafter, a uniform bio-Mg stent can be obtained directly by means of weaving technique according to the application requirements.

METHODS: The continuous Mg-6Zn alloy microwires were fabricated by a modified melt extraction method. The representative schematic diagram is shown in Fig. 1a. The extraction rates were 20 m/s, 30 m/s and 40 m/s, respectively. The microstructural investigations were performed using SEM. The calorimetric response of the as-cast alloy and the mirowire were measured using DSC. The phase compositions were identified by XRD. The mechanical properties were investigated comparatively at room temperature. The degradation behaviours were studied under simulated body environment. The degradation mechanisms were analyzed based one EIS measurements.

RESULTS: A circular configuration microwire is achieved when the extraction rate of is over 30 m/s. The Mg-6Zn based microwire is composed of Mg matrix and an amorphous phase, and exhibits higher basal texture than that of as-cast sample. The yield strength and ultimate tensile strength of the Mg-6Zn based microwire by 40 m/s extraction rate at room temperature are 401 MPa and 447 MPa, respectively, which are 3.11 and 2.56 times higher than those of as-cast ingot correspondingly.

In addition, it has been found that a low degradation rate of 0.321 mm/y is attained in a simulated body fluid, which is less than 1/10 of that of as-cast sample. The EISs results show that the as-cast ingot is mainly composed of a capacitive loop in high to medium frequency and an inductive loop in medium to low frequency. The equivalent circuit model of $R_s(C_{dl}R_{ct})$ (LR_L). Conversely, the EISs of microwire are composed of two capacitive loops in high and medium frequency ranges. The equivalent circuit model is $R_s(C_{dl}\ R_{ct})$ $(C_f\ R_f)$.

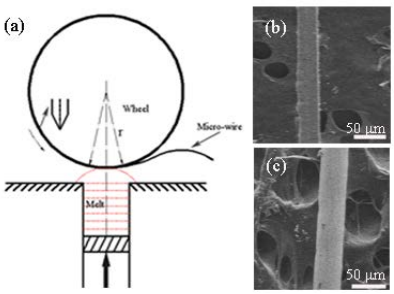

Fig.1. (a) Schematic diagram of a modified melt extraction method; (b) 20 m/s; (c) 30 m/s

DISCUSSION & CONCLUSIONS: A uniform Mg microwire is prepared firstly by a modified melt extraction method. The strength is improved by solid solution strengthening, fine grain and amorphous phase. The corrosion is improved by the reduced pitting corrosion and a compact oxide film.

REFERENCES: [1]M Movahed et al (2006). *J Invasive Cardiol.* **18**, E198-202.

ACKNOWLEDGEMENTS: It is supported by NSFC (51101142;50821001) and NCET-12-0690.

Amorphous alloys – processing, properties and applications

K J Laws[1,2], J D Cao[1,2], M Ferry[1,2]

[1]*Australian Research Council Centre of Excellence for Design in Light Metals, Australia*

[2] *School of Materials Science and Engineering, University of New South Wales, Sydney, NSW 2052, Australia*

INTRODUCTION: Amorphous Alloys and Bulk metallic glasses (BMGs) are multicomponent metal alloys that form a glassy structure with relative ease upon cooling. The amorphous nature of BMGs imparts exceptional mechanical properties, often surpassing those of conventional metal alloys which have generated considerable interest in both the technological and research arenas. Unique to the vitreous state, these alloys exhibit a glass-transition (temperature) similar to polymers and ceramic glasses whereby the vitreous solid relaxes into a supercooled liquid state, leading to a dramatic decrease in viscosity. This extreme softening behaviour allows novel thermoplastic forming processes to be carried out, that are simply unachievable among conventional metal processing methods [1]. Further, the structure of amorphous alloys is completely homogeneous leading to highly tailorable mechanical and corrosion/absorption rate properties as implant materials. Notably the magnesium-zinc-calcium amorphous alloys are completely resorbable [2,3]. These unique alloys, specifically focussed on implant device fabrication will be discussed in detail.

METHODS: A range of BMG alloys belonging to the Mg-Zn-Ca system which has been found to be completely bioresorbable have been produced at UNSW. All alloys are prepared from high purity (99.95wt% or better) Mg, Zn and Ca. These components are alloyed and cast into various pre-forms using an injection casting technique [4]. Thermoplastic forming properties of these alloys were determined using Differential Scanning Calorimeter (Netzsch DSC 204 F1) and Dilatometer (Netzsch DIL 402C). Electrochemical tests were performed using a three-electrode flat-cell (Princeton Applied Research). The cell contained 300 mL of minimum essential medium (MEM, Gibco 56416C) as the electrolyte in this study [2].

RESULTS: Potentio-dynamic testing in MEM showed rapid dissolution rates of Ca-rich amorphous alloys within this system when compared to Mg-rich amorphous alloys. However, Ca-rich amorphous alloys showed significantly superior processability within the supercooled liquid region compared to Mg-rich amorphous alloys. Figure 1 shows a prototype threaded section of an orthopaedic implant device forged in the supercooled liquid state.

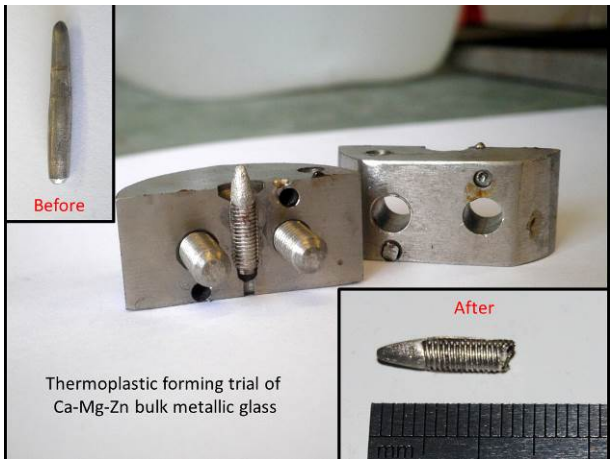

Fig. 1: Images of a bioresorbable BMG prototype fixation component formed in the supercooled liquid region at a temperature of 120°C.

DISCUSSION & CONCLUSIONS: Specific amorphous alloys from the Mg-Zn-Ca alloy system have been shown to be biocompatible [3]. Proof of concept bio-devices were successfully fabricated by superplastic forming processes within the supercooled liquid state of Mg-Zn-Ca BMG alloys. High tolerance feature replication and improved mechanical properties were observed after superplastic forming as a supercooled liquid.

REFERENCES: [1] J Schroers (2010) *Advanced Materials* 22: 1566–97. [2] JD. Cao, NT Kirkland, KJ Laws, N Birbilis, M Ferry (2012) *Acta Bio* **8**:2375-83. [3] B Zberg, PJ Uggowitzer, JF Löffler (2009) *Nat. Mater.* 8:887–91. [4] KJ Laws, B Gun, M Ferry (2008) KJ Laws, B Gun, M Ferry *Mat. Sci. Eng. A* **475**:348-54.

ACKNOWLEDGEMENTS: Australian Research Council Centre of Excellence for Design in Light Metals (CE0561574) for funding this work.

Fe-based alloys with TWIP effect for biodegradable stents

E Mouzou[1], P Agung[1], A Mostavan[1] C Paternoster[1], R Tolouei[1], S Turgeon[1], D Dubé[1], F Prima[2], D Mantovani[1]

[1]Lab. for Biomaterials & Bioengineering (CRC-I), Dept. Min-Met-Materials Engineering & University Hospital Research Centre, Université Laval, Québec City, Canada. [2]Laboratoire de Physicochimie de l'École Nationale de chimie de Paris.

INTRODUCTION: Iron-based alloys have shown to possess appropriate mechanical properties for cardiovascular stents applications if compared to that of stainless steel. However, the corrosion rate is still considered slow for most applications. Although interesting strategies such as the addition of alloying elements and the modification of the microstructure have been investigated, they did not achieve yet the appropriate corrosion rate matching the arterial remodeling. Moreover, reducing the material volume and the strut thickness are recognized clinical targets. In another context, Fe-Mn-C alloys with TWIP effect are largely used in the automotive industry for their exceptional high strength and deformation [1]. The aim of this research was to investigate the potential for these alloys to present i) suitable mechanical properties while reducing strut thickness; ii) uniform corrosion at a rate matching the remodeling process of the artery.

MATERIALS AND METHODS: Specimens of Fe-Mn-C steel with TWIP effect were produced industrially in the form of ingots (Arcelor Mittal, Belgium). Rolling and heat treatments were applied in our laboratory to industrial ingots. Different kinds of thermo-mechanical (TM) treatments were applied to generate differents microstructures and textures. Optical Metallography (OM), Scanning Electron Microscopy (SEM) and X-Ray diffraction (XRD) were used to investigate microstructures and textures. Potentiodynamic polarization and static degradation tests in Hank's solution were carried out on the alloy to assess the corrosion forms and rates. Finally, the biological performances of the specimens were assessed by smooth muscle cell viability studies.

RESULTS: Optical microscopy of the cold-rolled and recrystallized sheets of this alloy showed equiaxed grains with an average size of 9µm. SEM and XRD revealed the presence of the austenite and ferrite and intermetallic phases containing Al. Potentiodynamic polarization tests in a modified Hank's solution gave a corrosion rate of 0.29mm/year. After 24 and 48 h of culture, smooth muscle cell viability was inhibited on Fe-Mn-C if compared to the control, similarly to what happened on casted or electroformed pure iron**.**

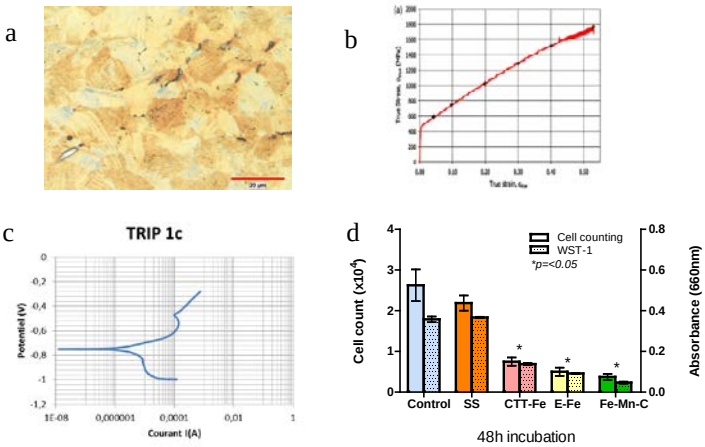

Figure 1: a) microstructure, b) tensile test [1], c) potentiodynamic polarisation test, d) cell viability.

DISCUSSION & CONCLUSIONS

The potentiodynamic corrosion test showed a corrosion rate of 0.29mm/year, thus confirming the results obtained by Hamada et al. [2]. Cell viability tests showed that the alloy inhibits the smooth muscle cells activity as well as the electroformed E-Fe and CTT iron [3]. Further works will focus on the optimization of TM processing parameters. They are expected to modulate the mechanical properties, the corrosion rate and the biocompatibility of this new family of biodegradable metals.

REFERENCES: [1] S. Allain et al (2004) Materials Sci. & Eng.; [2] A.S. Hamada et al (2007) Acta. Uni. Oul.**;** [3]M. Moravej et al (2010) Acta Biomaterialia.

ACKNOWLEDGEMENTS: The authors would like to thank M. Choquette Ph.D, A. Ferland, V. Dodier, D. Marcotte, and M. Larouche, of Min-Met-Materials Eng at Université Laval. The also acknowledge ACDI and PCBF for scholarship.

Effect of phosphorus on the corrosion behaviour of electroformed iron-based bilayer materials targeted for biodegradable stent application

A Mostavan, C Paternoster, R Tolouei, E Ghali, D Dubé, D Mantovani

Lab. for Biomaterials & Bioengineering (CRC-I), Dept. Min-Met-Materials Engineering & University Hospital Research Centre, Université Laval, Québec City, Canada

INTRODUCTION: Biodegradable iron-based alloys are potential candidates to permanent cardiovascular devices due to their good biocompatibility and mechanical properties in spite of their slow degradation rates [1]. Electroforming has been already proven to be an effective and versatile method to produce metallic stent, as it has the potential to fabricate tubes with suitable properties [2]. Phosphorus has been selected as alloying element in iron due to its beneficial effect on biological and mechanical strength. Moreover, phosphorus has been investigated to accelerate the corrosion rate of iron in simulated body fluid (SBF) & HCl [3,4]. The objective of the present work is to investigate the effect of phosphorus on corrosion behaviour of electroformed iron and iron-phosphorus (Fe/FeP multilayers).

METHODS: Fe/FeP multilayers were prepared by a dual bath electroforming technique. It consists of two electrolytes containing iron and iron-phosphorus alloy, respectively, and one rinsing bath. The process parameters such as current density and electrolyte concentration were optimized to have Fe/FeP bilayer. Electron probe microanalysis (EPMA) and scanning electron microscope (SEM) were respectively used to study the elemental distribution and microstructures of multilayer. The potentiodynamic polarization tests as well as static immersion test have been conducted to evaluate the effect of phosphorus on corrosion properties and degradation behaviour in the Hank's solution.

RESULTS: The bilayer Fe/FeP was obtained at current density of $2Adm^{-2}$ for 4 hours (3h for forming of Fe layer and 1h for forming of FeP layer). The results indicate that the thickness and concentration of the deposited iron phosphorus layer can be controlled by current density and electrolyte concentration. Figure 1 shows the elemental distribution in cross-section of Fe/FeP bilayer.

The potentiodynamic polarisation tests have revealed that the corrosion rate of iron phosphorus was higher (1.74mmpy) than the one of pure iron layer (0.99mmpy). Moreover, the immersion test displayed slight differences between electroformed Fe/FeP (0.30mmpy) and electroformed pure Fe (0.26mmpy).

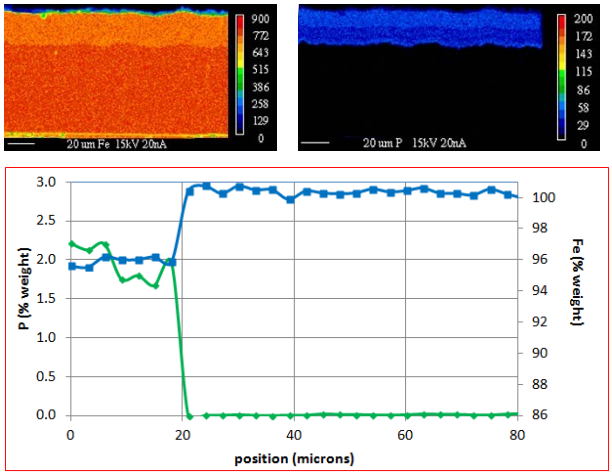

Fig.1. Elemental distribution of iron and phosphorus in electroformed Fe/FeP bilayer.

DISCUSSION & CONCLUSION:
Current density and electrolyte composition were carefully chosen to optimize the electroforming of bilayer Fe/FeP specimens. The current density influences the thickness and microstructure of Fe and FeP layer. The concentration of iron chloride and sodium salt of phosphoric acid in FeP deposition bath was optimized in order to attain phosphorus content of about 2 wt%. The corrosion test showed that addition of phosphorus accelerates the corrosion rate of iron. During immersion test, it is probable that galvanic corrosion occurs between the two layers of electroformed Fe/FeP which contact together in solution and the effect of corrosion product inhibited degradation rate.

REFERENCES: [1]Peuster et al., Heart, 2001. 86(5): p. 563-569. [2]Moravej et al, Acta Biomaterialia, 2010. 6(5): p. 1726-1735. [3]Wegener et al., Materials Science and Engineering: B, 2011. 176(20): p. 1789-1796. [4]Foroulis et al., Journal of the Electrochemical Society, 1965. 112(12): p. 1177-1181.

ACKNOWLEDGEMENTS: The authors acknowledge the kind technical collaboration of M. Choquette Ph.D, A. Ferland, V. Dodier, D. Marcotte, M. Larouche, of the Dept. of Min-Met-Materials Eng at Université Laval.

Development of PLGA-infiltrated porous iron for temporary medical implants

AH Yusop, NM Daud, H Hermawan

Faculty of Biosciences and Medical Engineering, Universiti Teknologi Malaysia (UTM), Malaysia

INTRODUCTION: Almost all studies on iron (Fe) as biodegradable metal concluded that a faster degradation rate is desired [1]. Biodegradable poly(lactic-*co*-glycolic) acid (PLGA) can be used as an accelerator for Fe degradation. This work aims to develop PLGA-infiltrated porous Fe (PIPI) as a new composite with tailored degradation rate. Its mechanical and degradation properties including the cell viability will be assessed.

METHODS: Open-pore Fe foam sheet (pore size 450 µm) was provided by Alantum, Korea. PLGA (Lactel, USA) with 50:50 molar ratio and inherent viscosity of 0.38 dl/g was dissolved in trichloromethane and was infiltrated into the Fe pores using the vacuum impregnation technique at -0.7 MPa for 20 minutes to form full-dense PIPI. Compressive test, static immersion degradation and cell viability test (MTT assay) using human skin fibroblast (HSF) cells were conducted on direct contact with the PIPI samples. Fe ions concentration was determined by using AAS.

RESULTS: Table 1 shows that mechanical properties of the PIPI samples were slightly inferior to those of pure Fe.

Table 1. Mechanical properties of the samples.

Unit in MPa	Pure Fe	PIPI
Compressive strength	0.22 ± 0.01	0.20 ± 0.01
Yield strength	0.18 ± 0.01	0.15 ± 0.01
Modulus of elasticity	25 ± 3.07	23 ± 5.25

Figure 1 shows that Fe^{2+} concentration and weight loss percentage of the PIPI samples were higher than those of pure Fe after the immersion test.

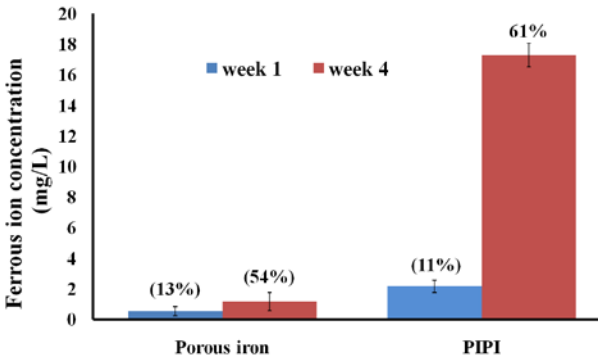

Fig. 1: Mass losses and Fe^{2+} concentration of pure Fe and PIPI samples.

Figure 2 shows that the HSF cell viability of the PIPI samples was slightly higher than that of pure Fe.

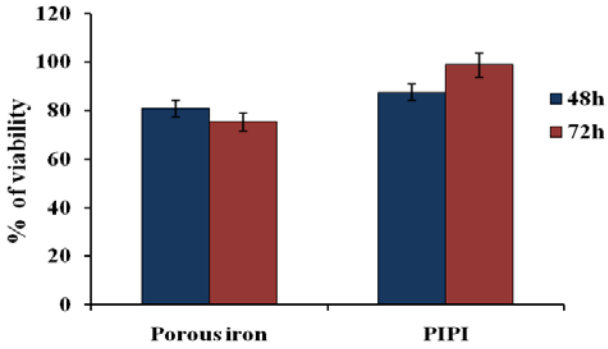

Fig. 2: Viability of HSF 1184 cells after 48 h and 72 h incubation on pure Fe and PIPI samples.

DISCUSSION & CONCLUSIONS: Results from the compression test (Table 1) indicate that the existence of PLGA in the PIPI slightly reduced the original strength of the Fe foam. The PLGA has lower strength than Fe and hence the strength of the PIPI composite was slightly reduced [2-3]. Degradation rate of PIPI samples was higher than the pure Fe foam (Fig. 1) as measured via mass losses and Fe^{2+} concentration. This was expected as the degradation of PLGA, which is faster than Fe, created acidity that dissolved Fe-oxide layer and thus promoted further Fe degradation. The MTT assay (Fig. 2) shows that PIPI has higher cell viability of HSF compared to pure Fe indicating a positive effect of PLGA degradation on the HSF cell viability [3]. Based on the above three assessments, it is concluded that incorporating biodegradable polymers into biodegradable metals (PLGA into porous Fe) could become a potential alternative strategy to tailor the degradation behaviour of Fe.

REFERENCES: [1] H. Hermawan (2012) *Biodegradable Metals: From Concept to Applications*, Springer. [2] L.S. Nair and C.T. Laurencin (2007) *Prog Polym Sci* **32**:762-36. [3] L.D. Wegner and L.J. Gibson (2001) *Int J Mech Sci* **43**:1061-11. [4] L. Lu, S.J. Peter and M.D. Lyman (2000) *Biomaterials* **21**:1837-8

ACKNOWLEDGEMENTS: Malaysian Ministry of Higher Education and UTM (FRGS R.J130000.7836.4F123).

Synthesis of bovine hydroxyapatite-iron composite via dry mechanochemical process for biodegradable bone scaffolds

JA Nordin[1], NM Daud[1], DH Prajitno[2], H Nur[3], H Hermawan[1]

[1] *Faculty of Biosciences and Medical Engineering, University Teknologi Malaysia (UTM), Malaysia.* [2] *Indonesian Nuclear Research Agency (PTNBR-BATAN), Indonesia.* [3] *Ibnu Sina Institute for Fundamental Studies, UTM, Malaysia.*

INTRODUCTION: Hydroxyapatite (HAp) is widely used in orthopedic and dental surgeries [1]. This study aims to synthesize a Fe-reinforced natural HAp composite via dry mechanochemical process without chemical addition. An improvement to the mechanical strength and cytocompatibility is expected with the presence of Fe ions in the HAp structure.

METHODS: Samples of a bovine cortical bone were cut, washed and boiled for 24 h to remove impurities. They were deproteinized at 160°C for 48 h and calcinated at 750°C for 6 h to obtain bovine HAp powders (HAp(B)). A composite of HAp-30wt% Fe (HAp(B)+Fe) was prepared by mixing HAp(B) and pure Fe powders (Goodfellow, UK) using high energy milling for 3 h in a Teflon vial with Zirconia balls. The charge to ball ratio and rotational speed were 1:10 and 1200 rpm, respectively. Pellets (∅ = 8 mm, thickness = 5 mm) were compacted at 129 kg.cm^{-2} and sintered at 900°C for 2 h. Characterization was done using XRD, FTIR, and SEM, while a hardness Vickers test was carried out using a 10 kgf-load. The cytotoxicity test was carried out using human mesenchymal stem cell (HMSC) following the ISO 10993-12. The MTT assay was used to measure the cell viability after 24 h.

RESULTS: Figure 1 shows the FTIR spectra identifying the substitution of Fe in the HAp(B).

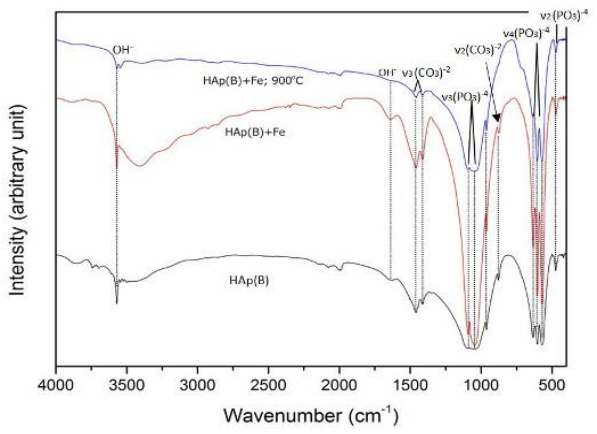

Fig. 1: FTIR spectra of the HAp(B) and the HAp(B)+Fe composite.

The hardness of the HAp(B) pellets was 54.15 Hv, while the HAp(B)+Fe was 108 Hv. The XRD pattern identified the presence of HAp (JCPS 9-0432), crystalline Fe (JCPS 6-0696) and Fe_2O_3 (JCPDS 033-0664) on the HAp(B)+Fe but no change on that of the HAp(B). The MTT result showed the percentages of cell viability of 88% and 87% for HAp(B) and HAp(B)+Fe, respectively. The viability of HAp(B)+Fe was 80% higher than the control.

DISCUSSION & CONCLUSIONS: The FTIR peaks at 1415 and 1459 cm^{-1} correspond to ν_3, and a band at 871 cm^{-1} corresponds to ν_2, indicating the stretching vibration of carbonate groups. A sharp peak was defined after the HAp(B) was milled with the Fe addition. The sintering at 900°C caused a disappearance of hydroxyl peak at 1638 cm^{-1}. Additional 3 peaks observed at 633, 602 and 568 cm^{-1} corresponds to ν_4 of phosphate [2]. The addition of Fe increased the hardness of HAp(B) by two fold due to the presence of Fe^{3+} in the HAp lattice structure that increases its crystallinity [3]. The MTT assay demonstrated that the presence of Fe in the composite was not toxic to HSMC and the HAp(B) gave higher percentage of the viability compared to the synthetic HAp. Other work found that bovine HAp increased osseoconduction at 12 weeks compared to the synthetic one [4]. It was also observed that the released Fe ions into the medium accelerated the precipitation of Ca^{2+} and PO_4^+ on the surface of the composite. The addition of 30wt% Fe into bovine HAp has improved its hardness and cytocompatibility.

REFERENCES: [1] V.S. Chandra, G. Baskar, R.V. Suganthi, et al (2012) *ACS Appl Mater Interfaces* **4**:1200-10. [2] I. Rehman and W. Bonfield (1997) *J Mater Sci Mater Med* **8**:1-4. [3] J. Wang, T. Nonami and K. Yubata (2008) *J Mater Sci Mater Med* **19**:2663-7. [4] H. Sano, K. Shibasaki, T. Matsukubo, et al (2002) *Bull Tokyo Dental Coll* **43:**75-82.

ACKNOWLEDGEMENTS: Malaysian Ministry of Higher Education and UTM (FRGS R.J130000.7836.4F123), and PTNBR-BATAN, Bandung, Indonesia.

Stent materials-dependent macrophage fusion and secretion of inflammatory cytokine and chemokine

L Mao[1,2], M Kwak[2], Q Xue[2], Y Lu[2], J Niu[1], J Zhang[1], G Yuan[*1], R Fan[*2]

[1] *School of Materials Science and Engineering, Shanghai Jiao Tong University, Shanghai 200240, China.* [2] *Department of Biomedical Engineering, Yale University, New Haven, CT 06511, USA.*

INTRODUCTION: By virtue of the versatility and intimate relationship with implanted materials, macrophage has been implicated as a pivotal cell in both wound healing of tissues around implant and in the pathogenesis of implant failure[1-2]. Foreign body giant cell (FBGC) formation from the fusion of macrophages is a hallmark feature of chronic inflammation due to the persistent presence of a non-phagocytosable foreign body[3]. Here we report on the study of macrophage adhesion, activation and fusion to form FBGC, and their secretory profile expression by assessing the production of inflammatory cytokine and chemokine on biodegradable and non-biodegradable cardiovascular stent substrates to develop a better understanding of FBGC formation and function, with the ultimate goal being the inhibition of FBGC formation and its potential adverse effects.

METHODS: The ingots of Mg-2.5Nd-0.2Zn-0.4Zr (wt%, hereafter, denoted as JDBM) alloy were manufactured by solution treatment (T4) followed by extrusion and annealing. 316L stainless steel was obtained from commercial sources. Macrophages adhesion and fusion were investigated by culturing macrophages directly on degradable and non-degradable substrates with cell density of 4×10^5/ml. The adherent cells were double-stained with Phalloidin and DAPI. The production of inflammatory cytokine/chemokine was quantified with sandwich enzyme-linked immunosorbent assays (ELISA).

RESULTS: Degradable stent substrate JDBM promoted significantly decreased levels of macrophage adhesion and macrophage fusion when compared to non-degradable 316L stainless steel, as illustrated in Fig. 1. Inflammatory cytokine and chemokine expression were also dramatically influenced by substrate. Pro-inflammatory cytokines IL-1 β， IL-6 and TNF- α expression by biomaterial adherent macrophages/FBGCs vary between the degradable and non-degradable substrates, indicating biomaterial dependent levels of cell activation. This result clearly demonstrated that material surface exerted a profound effect on macrophage adhesion, FBGC formation and cytokine/chemokine profiles derived from activated macrophages and FBGCs adherent to substrates.

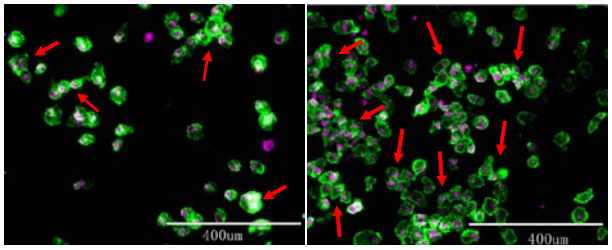

Fig. 1: Induction of macrophage fusion on degradable JDBM (a) and non-degradable 316L stainless steel (b) substrates. Arrows indicate FBGC derived from macrophage fusion.

DISCUSSION & CONCLUSIONS: The host inflammatory reaction is a normal response to injury and synthetic biomaterials, which are apparently not immunogenic in the classic adaptive sense. Foreign body giant cell (FBGC) derived from macrophage fusion is a prominent cell type on retrieved cardiovascular stents and is observed as a result of the inflammatory response induced by implants and other foreign bodies. Studies presented in this work illustrate the nature of cell/substrate interactions that support macrophages adhesion, activation, fusion to form foreign body giant cells, and their secretory profile production which may be significant to the eventual biocompatible outcome. Information and perspectives gained from this study will provide biologically derived criteria for improved stent material design which will modulate immune cell/surface interactions, and accordingly, to an understanding of the physiological roles of foreign body giant cells at sites of chronic inflammation.

REFERENCES: [1]W. J. Kao, D. Lee (2000) *Biomaterial* **22**: 2901-2909. [2]P. Thomsen, C. Gretzer (2001) *Curr. Opin. Solid State Mater. Sci.* **5**: 163-176. [3]J. M. Anderson, K. Defife, A. Mcnally et al (1999) *J Mater Sci-Mater M* **10**: 579-588.

Microstructure, mechanical properties and corrosion behaviour of Mg-3Al-1Zn alloy stent tubes

K Hanada[1], X Huang[2], K Matsuzaki[1]

[1]*Advaced Manufacturing Research Institute, National Institute of Advanced Industrial Science and Technology (AIST), Japan.* [2]*Materials Research Institute for Sustainable Development, National Institute of Advanced Industrial Science and Technology (AIST), Japan.*

INTRODUCTION: Mg alloy tubes are required to have appropriate biodegradability and mechanical properties for stent application [1], and these properties are affected by microstructures. The Mg alloy stent tubes, which are fabricated through repeated drawing and heat treatment, have different microstructures definitely from cast or extruded or rolled alloys [2,3]. Therefore the characterization of the stent tubes is essential to understand the stent performance. In this study, the microstructure, the mechanical properties and corrosion behaviour of Mg-3Al-1Zn (AZ31) alloy stent tubes were investigated.

METHODS: AZ31 billet of commercial purity was extruded into a thin-walled long tube (ϕ3.0mm ×ϕ2.6mm×L1000mm) at 723 K with an extrusion ratio of 68:1 and was annealed at 573 K for 30 min. The AZ31 alloy stent tubes (ϕ1.8mm×ϕ1.5mm ×L300mm) were fabricated by repeated cold drawing and annealing of the obtained tube, and then the grain structures were controlled by changing deformation mode and annealing temperature in the last processing.

The microstructure and mechanical properties of the stent tubes was examined by optical microscopy and tensile measurement, respectively. The #4000-polished stent tubes (ϕ1.8mm×ϕ1.5mm×L7mm) were immersed in a simulated body fluid (SBF) at 310 K for 18 hours, and the corrosion behaviour was examined.

RESULTS: Figure 1 shows the influence of grain size on the mechanical properties of the stent tube. The UTS and 0.2% proof stress decreased with increasing the mean grain size of the stent tube, and the elongation was slightly improved at the mean grain size of 12-15 μm.

Figure 2 shows the appearances of the stent tubes after the immersion test in SBF. The stent tube with the mean grain size of 14.2 μm maintained most of its original shape; on the other hand, the tube with the mean grain size of 18.2 μm was locally corroded. Those weight loss rates were 1.1 mg/cm^2/d and 5.3 mg/cm^2/d, respectively.

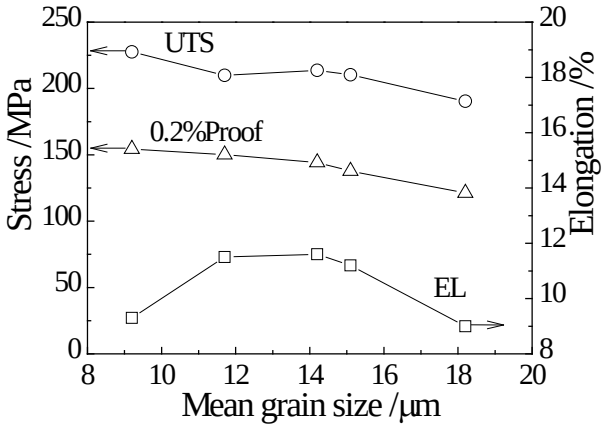

Fig. 1: Influence of grain size on the mechanical properties of AZ31 stent tubes.

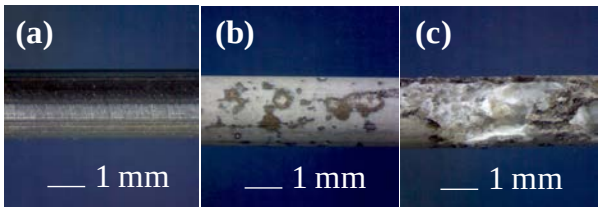

Fig. 2: Appearances of AZ31 alloy stent tubes: (a) as-polished tube, and as-immersed tubes with mean grain sizes of (b) 14.2 μm and (c) 18.2 μm.

DISCUSSION & CONCLUSIONS: The mechanical properties and corrosion behaviour of AZ31 stent tube is affected by the grain structure, and this indicates that the control of the grain structure in the stent tube fabrication is important for Mg alloy stent to show the required performance.

REFERENCES: [1] R.J. Werkhoven, W.H. Sillekens, J.B.J.M. Lieshout (2011) *Proc Magnes Technol*: 419-424. [2] Y.Z. Du, M.Y. Zheng, C. Xu, et al (2013) *Mater Sci & Eng A* **576**: 6-13. [3] X. Huang, K. Suzuki, A. Watazu, et al (2009) *Scripta Materialia* **60**: 964-967.

Surface structuring of AZ31 Mg alloy with a laser beam for biodegradable stent applications

AG Demir[1], B Previtali[1], V Furlan[1],

[1] *Department of Mechanical Engineering, Politecnico di Milano, Italy.*

INTRODUCTION: In biomedical applications functional surfaces are becoming accepted due to the advancements and availability of the new manufacturing methods in the industry. Among other methods, the use of a laser beam to structure surfaces is highly advantageous for industrial applications, since it is a highly flexible process generating both deterministic or stochastic patterns. In the case of biomedical applications, surface modifications can be exploited for the control of wetting behaviour, surface passivation and corrosion resistance, as well as control of the surface roughness for improved biocompatibility [1,2]. The proposed study investigates the use of a pulsed laser source operating in *ns* regime for the structuring of AZ31 Mg alloy, destined to be used on a biodegradable stent platform [3].

METHODS:

Laser surface structuring was studied with a pulsed active fibre laser with 1 mJ maximum pulse energy and 100 ns pulse duration on 0.4 mm thick AZ31 sheets. The laser beam was manipulated via a galvanometric scanner system, which housed a 100 mm focal lens. The focused laser beam had a diameter of 39 µm. Primarily the laser processing conditions were studied to opportunely regulate the surface roughness. The initial surface roughness of the cold rolled AZ31 sheets was R_a=0.26 µm. Through preliminary investigations it was determined that the surface roughness control was achievable through the laser beam-material interaction based on surface re-melting and re-solidification. For ns-pulsed laser source such conditions were applicable with low energy conditions, and highly defocused beam. Therefore, the laser fluence remains under the ablation threshold. If the interaction time is regulated, heat input can be manipulated to control the surface roughness (in range of parameters in Table 1).

Table 1. Process parameter window for the laser surface structuring of AZ31 Mg alloy

Focal position	f	2 mm
Pulse energy	E	0.10-0.25 mJ
Pulse repetition rate	PRR	20-70 kHz
Scan speed	v	25-100 mm/s
No. of passes	pass	1-4

RESULTS: The generated surface textures were characterized for their roughness with focus-variation based optical imaging. It can be seen that the R_a can be effectively controlled within the employed parameter range. Although surface roughness appears to be a useful parameter to distinguish surface texture, the surface topography present in the laser structured surfaces was found to be evidently different. Figure 1 depicts the smoothest (R_a=0.21 µm, R_z=1.30 µm) and roughest (R_a=4.44 µm, R_z=20.03 µm) surfaces generated within this study.

DISCUSSION & CONCLUSIONS: The results confirm the feasibility of surface structuring via a pulsed laser source, as effective change of surface roughness was achieved. Further study is being carried out on the extensive characterization of the surfaces for wetting behaviour, chemical composition, and mechanical resistance to wear.

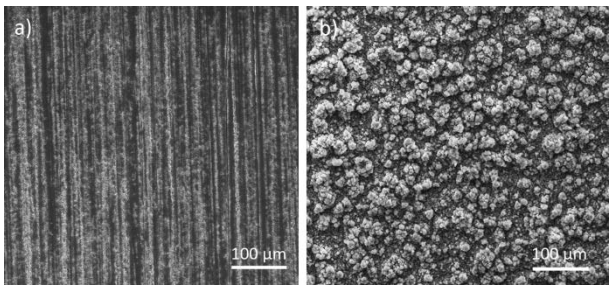

Fig. 2: Comparison of topographies achieved with the a) smoothest, and the b) roughest surfaces.

REFERENCES: [1] A. Kurella, N.B. Dahotre (2005) *Journal of Biomaterials Applications* **20** 5-50. [2] G. Nabucasagam, D. Dhinasekaran, A. Rajamanickam (2010) *Recent Patents on Corrosion Science* **2**, 40-54. [3] A.G. Demir, B. Previtali, Q. Ge et al, *Proceedings of the 1st International Conference on Design And Processes for Medical Devices*, pp. 35-38

ACKNOWLEDGEMENTS: The authors would like to express their gratitude to Fondazione CaRiTRO for partially funding the research under grant number 2011.0250.

Magnesium and its alloys – an introduction to their metallurgy and deformation behaviour

MV Manuel[1]

[1] *Department of Materials Science and Engineering, University of Florida, USA*

INTRODUCTION: As an anisotropic material, magnesium (Mg) displays unique deformation behaviors that fundamentally separate this class of materials from those with greater crystallographic symmetry, such as cubic materials. This lack of symmetry leads to the development to high internal stresses that manifests as twinning, slip, and ultimately grain boundary incompatibility that leads to poor ductility and localized strain with eventual failure. Thus, to design advanced Mg alloys and components made thereof, it is important to take in account all of these features. This presentation will provide an introductory level description of unit mechanisms and their mutual interactions that lead to various deformation processes. Topics are covered in a hierarchical fashion that starts with crystallography and includes elasticity, dislocation and twinning mechanics, grain boundary compatibility, solute chemistry effects, strengthening and softening mechanisms, and ending with fracture.

ACKNOWLEDGEMENTS: The author would like to gratefully acknowledge the National Science Foundation for their support under grant number DMR 0845868.

Mechanical properties and corrosion behaviour of ZK60 processed by ECAP for biomedical application

E Mostaed[1], Q Ge[1], M Vedani[1], PA De Oliveira Botelho[2], C Zanella[2], F Deflorian[2]

[1] *Department of Mechanical Engineering, Politecnico di Milano, Milan, Italy.*

[2] *Department of Industrial Engineering, University of Trento, Trento, Italy.*

INTRODUCTION: Magnesium alloys have been attracting much interest as candidates for vascular biodegradable stents due to their good biocompatibility and mechanical properties. However, their high inherent corrosion rate is an essential consideration. Previous studies proved that grain refinement of magnesium alloys leads to improve their mechanical properties as well as corrosion resistance [1, 2]. In this study, Equal Channel Angular Pressing (ECAP) was used to improve mechanical properties and corrosion resistance of ZK60 alloy through achieving an ultra-fine grain (UFG) structure. The mechanical properties, microstructural characterization, and corrosion behaviour before and after ECAP are presented.

METHODS: The experiments were conducted using a commercial ZK60 alloy in the form of extruded rods for ECAP process. Three steps of ECAP were performed for 4 passes at 250°C, 200°C, and 150°C, respectively. Microstructural characterization was performed by optical microscopy and field emission gun scanning electron microscopy on cross section of billets after ECAP. Mechanical properties after ECAP procedure were assessed on tensile test specimens with a gage length of 12 mm and the diameter of 4 mm, and micro hardness tests on both longitudinal and transversal section of the billet regions. The corrosion behavior of ECAP processed alloy was compared to that of as received coarse-grained materials by performing potentiodynamic polarization (0.166 mVs^{-1}) and open circuit potential (OCP) tests in phosphate buffered solution (PBS) of pH 7.4 and controlled temperature of 37°C.

RESULTS: Fig. 1 depicts the microstructure evolution from as-received ZK60 alloy to that of the alloys after 4 passes ECAP at 150°C. It is clearly seen from Fig. 1a that the as-received ZK60 features a bimodal grain structure, with coarse grains of ~ 20µm and fine grains of ~4µm, while after ECAP for 4 passes at 150°C (Fig. 1b), the ZK60 alloy shows a fully recrystallized grain structure with sub-micron grain size (the average grain size ~ 700 nm). The value of the yield strength, ultimate tensile strength, elongation to failure, and the hardness of the alloy corresponding to each step are listed in Table 1.

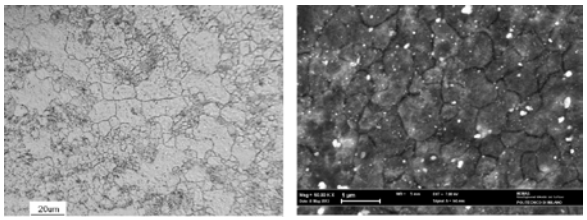

(a) As-received material (b)250°C 4passes+200°C 4passes+ 150°C 4passes

Fig. 1: microstructure improvement during ECAP.

Table 1. Mechanical properties of the ECAP processed ZK60.

Samples	Yield strength (MPa)	Ultimate tensile strength (MPa)	Elongation to failure (%)	Micro hardness (HV)
As-received	117	340	18.8	67.4
250°C 4 passes	NA	NA	NA	72.17
200°C 4 passes	114	275	28.8	74.6
150°C 4 passes	200	285	33.7	80.1

According to potentiodynamic measurements, inversion potentials and corrosion current densities are similar in both cases and are in the range of -1.5V vs. Ag/AgCl and 50µA/cm^2, respectively. Therefore, to make a clearer distinction, OCP results were compared, ECAPed sample showed a nobler behavior with an OCP of –1.46V vs. Ag/AgCl compared to –1.5V of as-received sample.

DISCUSSION & CONCLUSIONS: the influence of ECAP at three steps starting at 250°C and ending up at 150°C notably provided the achievement of ultra-fine grain structure. According to the table 1, during the procedure the yield strength and hardness of the alloy increased as well as the amount of elongation to failure corresponding to the ductility. In terms of corrosion resistance of the samples, OCP and potentiodynamic results revealed a nobler behavior of the UFG sample in the corrosive environment.

REFERENCES: [1] A. Yamashita, Z. Horita, T. G. Langdon.Mater. Sci. Eng. A. 300 (2001) 142-147. [2] G.R. Argade S.K. Panigrahi, et al. corrosion science 58 (2012) 145–151.

Effect of process on the properties of biodegradble Mg-2Zn-0.2Mn alloy

N Huang[1], SJ Zhou[1], LS Guo[1], J Wang[1]
[1]Key Lab. of Advanced Materials Technology, Ministry of Education, Southwest Jiaotong University, China

INTRODUCTION: Mg-based materials, as the most promising candidate of new generation biodegradable materials, have received considerable attention [1]. However, Mg alloy with suitable durability, mechanical property and biocompatibility still need to improve for the clinical requirements. In this work, controlling alloy element, grain size, cooling rate and extrusion temperature achieved to improve the above-mentioned properties.

METHODS: Mg-2Zn-0.2Mn was prepared by melting high purity Mg (99.999 wt%), Zn (99.999 wt%), Mg-Mn (3.4 wt% Mn) master alloy. Cast ingots were cooled in the furnace and water, respectively. Then the ingots were homogenized at 360 °C for 12 hours. Finally, the homogenized ingots were extruded at 230, 280 and 330 °C, with an extrusion ratio of 25:1 and a speed of 3mm/s. Tensile test was carried for mechanical property. Corrosion rate was evaluated by the immersion and electrochemical tests. Blood compatibility was evaluated by platelet adhesion and hemolysis ratio tests, and cell compatibility was studied by endothelial cells adhesion and apoptosis tests.

RESULTS & DISCUSSION:

Effect of Mn on the microstructure and properties: The grain size of Mg-2Zn-0.2Mn was decreased from ~10 to ~2 μm, which can be owe to the increasing of recrystallization temperature by doping of Mn. The dynamically recrystallized grain size cannot grow up during the extrusion process. The ultimate tensile strength (UTS) of Mg-2Zn-0.2Mn was increased from 237 to 317 MPa, as a joint contribution of solution strengthening and refined crystalline. Due to homogeneous microstructure of Mg-2Zn-0.2Mn, corrosion rate was decreased to 0.010 ml/d/cm^2.

Effect of cool rate on the microstructure and properties: With the increasing of the cooling rate of casting process, the grain size was significantly reduced from 200~400 μm at the traditional cooling rate in the furnace to 10~50 μm at fast cooling rate in the water, which is much favorite for further decreasing the crystal size through extrude process. The natural corrosion potential was also increased from -1.420 to -1.315 mV, and corrosion rate reduced as much as 10 times in the immersion test.

Effects of extrusion temperature on the microstructure and properties: The uniform isometric crystal with the grain size of 10~25 μm was obtained after extruded at 330 °C for Mg-2Zn-0.2Mn alloy fabricated by casting with slowly cooling. Its UTS was 225 MPa and corrosion rate was 0.012 ml/d/cm^2. Meanwhile, the UTS of alloys extruded at 230 and 280 °C were similar to that extruded at 330 °C, but corrosion rate was much higher than that extruded at 330°C. It is attribute to incomplete recrystallization, nonuniform grain size, and residual stress.

Biocompatibility of Mg-2Zn-0.2Mn: In Fig.1, significantly fewer platelets were adherent and activated on Mg-2Zn-0.2Mn surface than on the AZ31B alloy and 316L stainless steel (SS). And hemolysis ratio of Mg-2Zn-0.2Mn was 4.7%, which was much less than that of AZ31B (80.9%). Endothelial cells (EC) adhesion and proliferation behavior on Mg-2Zn-0.2Mn were superior to that on the AZ31B in apoptosis test (Fig. 2).

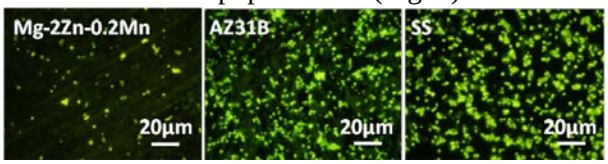

Fig. 1: Representative fluorescent images of adherent platelets on the samples incubated in platelet rich plasma for 45min.

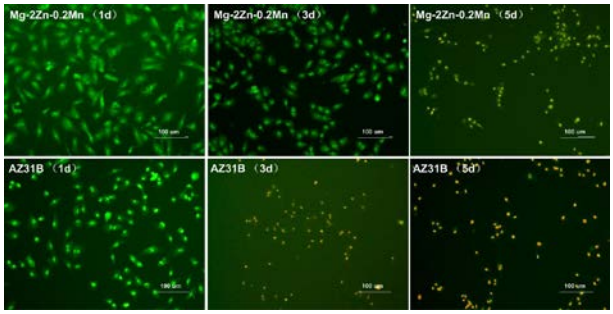

Fig. 2: Morphologies of EC in the immersing alloys solution with different time points after incubation for 1 day by stained AO/PI. Green: vital cells, red: dead cells.

CONCLUSIONS: Corrosion rate, mechanical property and biocompatibility of Mg-2Zn-0.2Mn were optimized by controlling alloy element, grain size, cooling rate and extrusion temperature.

REFERENCES: [1] M. Moravej, D. Mantovani. (2011) *Int J Mol Sci* **12**, 4250-70.

ACKNOWLEDGEMENTS: NSFC 81271701 and China Scholarship Council 201207000016.

Influence of different storage durations on the properties of degradable magnesium based implants

K Bracht[1], N Angrisani[1], JM Seitz[2], R Eifler[2], A Weizbauer[3], J Reifenrath[1]

[1] Small Animal Clinic, Veterinary University of Hannover, Foundation, Hannover, D, [2]Institute of Material Science, Leibniz University, Hannover, D, [3]Department of Orthopedic Surgery, Hannover Medical School, Hannover, D

INTRODUCTION: The storage of biomedical devices cannot be generally avoided. A possible influence of storage duration on structural changes of biodegradable magnesium based implants was discussed [1] but not proved yet. Therefore, aim of this study was to examine the storage influence on implant material and the corresponding impact on *in vitro* corrosion.

METHODS: Extruded cylindrical implants (n = 45, Ø 2.5 mm; 25 mm length) of LAE442 (approx. 90 wt% magnesium, 4 wt% lithium, 4 wt% aluminium and 2 wt% rare earth) were produced according to previously published studies [2]. Pins were randomly divided in three groups and were stored (dry, RT) for 0, 24 and 48 weeks. After the respective storage duration, pins were examined by three-point-bending (n=5), metallographic- and contrast analysis (n=5) as well as an *in vitro* corrosion test (n=5, pH buffered SBF for 8 weeks, 37°C with daily pH-control; change of SBF, when pH>8). After *in vitro* corrosion, µ-computed tomography and three-point-bending was performed. Statistical analysis was carried out by student´s t-test, significance level $\alpha = 0.05$.

RESULTS: Different storage durations did not have a significant effect on the implant stability. Also after *in vitro* corrosion, F(max) was in the same range for all storage durations, even though significantly lower than before *in vitro* corrosion (summed up; before: MV 160.45N, SD 3.25, after: MV 128.53N, SD 2.29). Corresponding to the results of three point bending, examinations with µCT80 also showed no significant differences in volume loss after the varying storage times, but between values assessed before and after *in vitro* corrosion (before: 122.72 mm^3; after, summed up: MV 106.26 mm^3, SD 0.56). Metallographic evaluation showed no clear differences in grain sizes between the pins after 0 weeks (MV 16.59±1.87µm) and after 48 weeks storage duration (MV 15.33±1.47µm). However, slight but significant higher values could be found for pins after 24 weeks storage duration (MV 17.79±1.88µm) (Fig. 1).

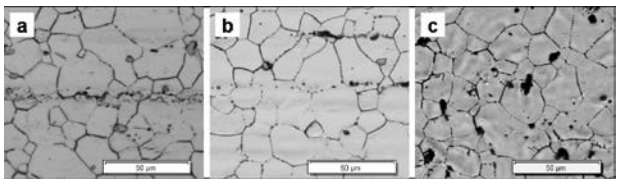

Fig. 1: Metallographic images: a) after 0w, b) after 24w, c) after 48w storage duration: grain sizes and precipitation analysis. Scale bar 50 µm.

Albeit not significantly, percentage precipitations (rare earths; lithium, aluminium (others)) measured in contrast analysis tend to increase with increasing storage duration (Tab. 1).

Tab. 1: Percentage precipitations after different storage durations

storage	0 weeks	24 weeks	48 weeks
rare earths [%] (MV±SD)	2.51 ± 1.22	2.08 ± 0.92	3.36 ± 0.94
others [%] (MV±SD)	4.30 ± 1.14	4.84 ± 1.52	5.31 ± 1.33

DISCUSSION & CONCLUSIONS: The present study shows that no significant changes of the implant properties occur during the storage of degradable LAE442 cylinders up to one year. The formerly described decrease in grain size after 24 weeks [1] could not be shown in this higher number of samples. However, since precipitations and grain sizes seem to alter slowly over time, storage durations longer than one year have to be examined to assess possible further changes.

REFERENCES:

[1] Ullmann B, Reifenrath J, Seitz JM, Bormann D, Meyer-Lindenberg (2013) *Proc Inst Mech Eng H.* 227(3):317-26. [2] Seitz JM, Collier K, Wulf E, Bormann D, Bach FW (2011) *Adv Eng Mater.* 13(9):B313-323.

ACKNOWLEDGEMENTS: The present study occurred within the CRC 599, which was funded by the German Research Foundation (DFG).

Degradation of Mg-Zn-Ca alloy processed by high pressure torsion for bone implant application in simulated body flood

GC Yue, SJ Zhu, LG Wang, X Ma, C Ji, SK Guan

School of Materials Science and Engineering, Zhengzhou University, 100 Kexue Road 450001, Zhengzhou, P.R.China

INTRODUCTION: The samples of biological medical Mg-Zn-Ca alloy were processed by high pressure torsion (HPT). It was shown that the sizes of grain and second phase were decreased to ~1.2μm and ~40nm separately after HPT, and the second phase distributed homogeneously in the grain interiors compared with the grain size of ~85μm and the second phase mostly distributed along the grain boundaries of as-cast alloy. Results of corrosion tests indicated that the corrosion rate was decreased while the degradation behavior changed from pitting corrosion to homogeneous corrosion in simulated body fluid.

METHODS:

Samples for high pressure torsion processing were prepared by cutting disks with a diameter of 10mm and a thickness of 1.2mm from the ingot. Then they were polished to final thickness of ~0.65mm. Then they were processed by high pressure torsion (HPT) to a total of 5 complete turns at a speed of 0.2rpm under an applied pressure, P, of 5GPa, thickness of the disk was decreased from 0.65mm to 0.3mm after HPT. Optical microscope and transmission electron microscope (TEM) were used to observe the microstructure evolution of the Mg-Zn-Ca alloy. While electrochemical and immersion tests in simulated body fluid were carried out to evaluate the corrosion properties.

RESULTS: The results indicate that after 5 turns of HPT the average grain size was decreased to ~1.2μm and the second phase particles were refined to nano-scaled while mostly distributed in the grain interiors (Fig.1a) under the interaction of mechanical refining and dynamic recrystallization refining. The electrochemical tests indicate that the E_{corr} decreased from -1.71V of as-cast alloy to -1.76V after HPT, because that the precipitation increased the relative surface of second phase particles which increased the number of micro-galvanic. While the I_{corr}, reduced from 1.91E-04 to 2.72E-06. Immersion tests indicated that the corrosion behavior changed from pitting corrosion to homogeneous corrosion in simulated body fluid, as illustrated in Fig. 1b. While the grain and second phase particles refinement with their homogeneous distribution might contribute to the homogeneous corrosion in SBF (Fig.2).

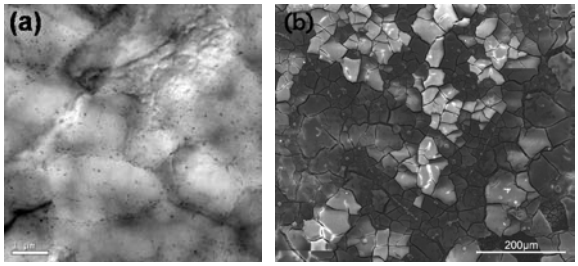

Fig. 1 (a) TEM image of samples after HPT and (b) SEM image after immersed into SBF for 48h

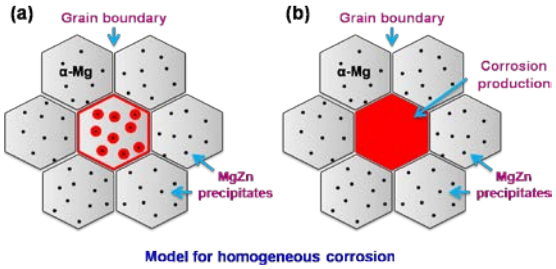

Fig. 2 Model for degradation behavior after HPT

DISCUSSION & CONCLUSIONS: After HPT processing, the grains were refined to ~1.2μm while the second phase particles were refined to ~40nm with a homogeneous distribution in the grain interiors due to the interaction of mechanical smashing and dynamic recrystallization. Corrosion tests showed that the corrosion properties were improved while the degradation behavior was changed from pitting corrosion to homogeneous corrosion in SBF.

REFERENCES: [1] Y. Xin, T.Hu, P.K. Chu. Acta Biomaterialia 7 (2011) 1452–1459. [2] Alexander P. Zhilyaev, Terence G. Langdon. Progress in Materials Science, 53(2008)893-979. [3] Pauline Serre, R.B. Figueiredo, et al. Materials Science and Engineering A528 (2011) 3601–3608.

ACKNOWLEDGEMENTS: The authors are grateful for the support by National Key Technology R&D Program (No.2012BAI18B01) and the National Natural Science Foundation of China (No.51171174).

Corrosion and wear behavior of Mg-xZn-0.8Zr alloy in simulated body fluid

D Liu*, L Liu, W Zheng, M Chen

School of Materials Science and Engineering, Tianjin University of Technology, Tianjin 300384, People's Republic of China

INTRODUCTION: In this work, Mg-xwt%Zn-0.8wt%Zr alloys (x=2.0, 2.5, 3.0, 4.0) used for bone implant were fabricated and the effects of content of Zn element on the mechanical properties of Mg-Zn-Zr alloys were investigated. In addition, there is inevitably micro-movement at the bone-implant interface *in vivo*. The wear behaviour of magnesium alloy in body fluid environment is not clear and corrosion process also have some impact on the wear behavior of magnesium. So it is necessary to study the corrosive wear behavior of the Mg-xwt%Zn-0.8wt%Zr alloys.

METHODS: High purity Mg (99.99%), high purity Zn (99.999%) and a high purity Mg–Zr master alloy were used to prepare Mg–xZn–0.8 Zr alloy. The electrochemical tests were performed using a three-electrode configuration. The friction and wear tests were implemented on a wear testing machine with a pin-on-disc contact configuration. The counterface was a stainless steel disc with a diameter of 80mm. The friction and wear tests were carried out under applied loads of 2N and 5N at a constant rotational velocity of 200r/min (linear speed of 0.65m/s). The tests were performed under deionized water, SBF lubrication and dry sliding condition, respectively.

RESULTS: As shown in Fig.1, with the Zn content increasing, wear loss of Mg-Zn-Zr alloys decrease gradually. At the same time, the wear loss of Mg-Zn-Zr alloys under dry sliding condition is lower than that of SBF lubrication, Fig.2 presents the wear surface morphology of the Mg-Zn-Zr alloys with different Zn content after wear testing under SBF lubrication. Some slight shallow grooves and corrosion products can be found on the worn surfaces.

DISCUSSION & CONCLUSIONS: The corrosion of the SBF makes the surface of the magnesium alloy loose and porous, and easily be worn away. At the same time, the magnesium alloy was vulnerable to scratch under load, and make the magnesium alloy easily corrode. The two influencing factors act on the magnesium alloy simultaneously, aggravated the wear of the magnesium alloy. Therefore , the wear rate of magnesium alloy under SBF lubrication is higher than that of under dry sliding condition .

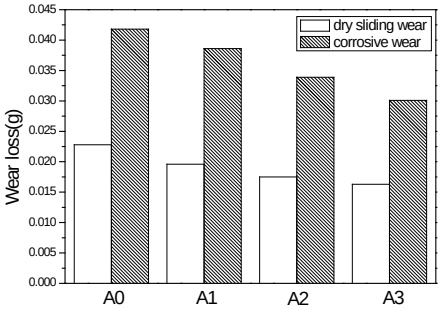

Fig. 1: Weight loss of the Mg-Zn-Zr alloys with different Zn content under dry sliding wear and corrosive wear condition

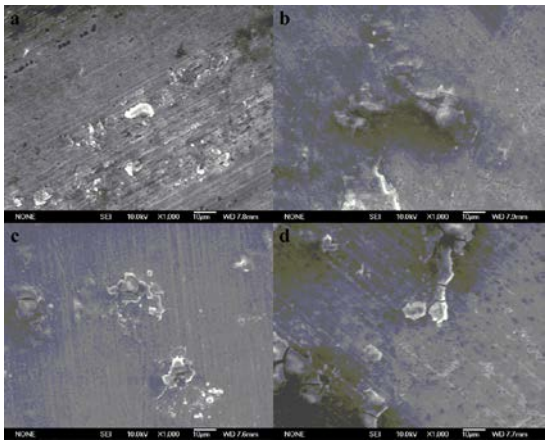

Fig. 2: Surface morphology of the Mg-xZn-Zr alloys with different Zn content after corrosive wear (a) x=2.0, *(b)* x=2.5, *(c)* x=3.0*and (d*) x=4.0

REFERENCES: *[1]Huang W.J., Lin Q., and Zhang X., Investigation of tribological properties of magnesium alloys under dry sliding and lubrication condition. Journal of Engineering Tribology , 2011,225(J1): 35.*

ACKNOWLEDGEMENTS: Acknowledgements The authors are grateful for the supports from the National Natural Science Foundation of China (No. 51271131).

Microstructures and corrosive properties in simulated body fluid of biological Mg-Zn-Y-Nd alloy by friction stir processing

SK Guan, SJ Zhu, LG Wang, GC Yue, J Wang, J Jin

School of Materials Science and Engineering, Zhengzhou University, 100 Kexue Road 450001, Zhengzhou, P.R.China

INTRODUCTION: The biomagnesium alloys, have been considered to be one of the most potential biodegradable metal materials due to its good mechanical compatibility, biological compatibility, biological security and biodegradable characteristics. However, the two major problems of poor corrosion performance in the environment of human body fluid or blood plasma and low mechanical properties prevent the development of biomagnesium alloys. In this study, the biological medical Mg-Zn-Y-Nd alloy with fine grain structures was modified by the friction stir process (FSP) technique.

METHODS:

Mg–Zn–Y–Nd alloy ingot was prepared with high purity Mg, high purity Zn, Mg–25Y (99.99wt.%) and Mg–25Nd(99.97wt.%) master alloys through induction of mild steel crucible at approximately 740 °C under CO_2/SF_6(vol.3000:1) atmosphere in an electronic resistance furnace. The cast ingots were homogenized with a heat treatment of 370 °C×12h, the sheets (10×60×75mm) were cut from the ingot by WEDM (wire cut electrical discharge machining) and rolled at 340 °C, then the specimens (Fig.1) were manufactured by FSP. The microstructure evolution of the stir zone of this alloy were studied by OM, XRD, SEM&EDS. The mechanical properties and corrosion properties of this alloy after FSPed process was studied by tensile tests, electrochemical experiments and pH changes during immersion tests.

Fig.1 Specimens manufactured by FSP

RESULTS: The result indicate that, because of the dynamic recrystallization occurred during FSP under the interaction of severe plastic deformation and thermal cycle, the microstructure of alloy by FSPed is homogeneous and consists of fine recrystallized equiaxed grains with ~2μm in size (Fig.2(a)), and the second phase particles became extremely small during FSP and distributed dispersedly in the grain interiors (Fig.2(b)). The alloy obtained good comprehensive mechanical properties by FSPed. The microhardness is 75HV, the ultimate tensile strength is 238MPa and elongation is 31%. The corrosion resistance of alloy was improved. The corrosion potential of alloy by FSPed increased from -1.745V to -1.7219V, and the corrosion current density decreased from 4.37×10^{-4}A/cm^2 to 4.01×10^{-4}A/cm^2 comparing with as-cast alloy. Because of obtaining fine grain and homogeneous microstructure, the improvement of mechanical properties, uniform corrosion performances and decrease of corrosion rate will provide theoretical ground for Mg-Zn-Y-Nd alloy as vascular stent application.

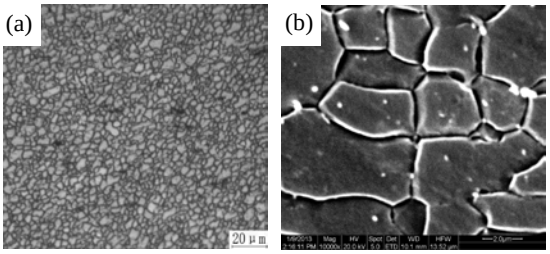

Fig.2: optical image (a) and SEM micrograph (b) of FSP alloy

CONCLUSIONS: After FSP treatment, the stir zone consists of fine equiaxed recrystallization grains. The second phase distributed along grain boundaries in as-cast state was broken into fine, uniform particles during the deformation and dispersed in the grains. The alloy obtained good comprehensive mechanical properties. The electrochemical measurement and pH value variety with immersion time in simulated body flood showed that the FSP treatment can obviously improve corrosion resistance of Mg-Zn-Y-Nd alloy.

ACKNOWLEDGEMENTS: The authors are grateful for the support by National Key Technology R&D Program (No.2012BAI18B01) and the National Natural Science Foundation of China (No.51171174).

Selective laser melting of biodegradable metals

L Jauer[1], W Meiners[1], R Poprawe[2]

[1] *Fraunhofer Institute for Laser Technology ILT, Aachen, Germany* [2] *Chair for Laser Technology LLT, RWTH-Aachen University, Aachen, Germany*

INTRODUCTION: Additive manufacturing technologies (often also referred to as 3d printing) such as Selective Laser Melting (SLM) [1] belong to an emerging field of manufacturing technologies. Due to its high degree of design freedom, SLM enables the generation of individualized implants (e.g. for cranio maxillofacial applications) or implants with defined cellular structures (e.g. acetabular cups or scaffolds). Especially for biodegradable implants, building defined interconnected cellular structures may be beneficial. These structures would allow a full vascularization of the implant and the ingrowth of new bone tissue throughout the whole implant. Thereby, corrosion products can be removed more efficiently and the implant is strengthened during the degradation process.

METHODS: During this study, a laboratory SLM-machine setup was used. The laser beam of a single mode ytterbium fiber laser (IPG YLR-200) with 200W maximum output power is deflected and focused by a galvanometric scanner (SCANLAB hurrySCAN 20/30) with a 254mm focal f-theta lens (SILL S4LFT 3254/126) resulting in a beam diameter of approx. 100µm in the focal plane. The process chamber enables processing in an inert gas atmosphere, which is composed of argon and helium, with oxygen content below 50ppm. The used materials are gas atomized powders with spherical particle shape. Fe35Mn (Nanoval) as well as AZ91 (Zentrum für Funktionswerkstoffe) powders are sieved to particle sizes smaller than 90µm before SLM processing. To build various SLM test specimen, the main SLM process parameters such as laser power, scan speed, hatch distance and exposure strategy are varied.

RESULTS: Simple test specimens with densities greater than 99% were manufactured from both iron based (Fe35Mn) and magnesium based (AZ91) alloys. Fig. 1 exemplarily shows a picture of a polished cross-section of a Fe35Mn SLM test specimen taken by light microscope (left) and scanning electron microscope (right).

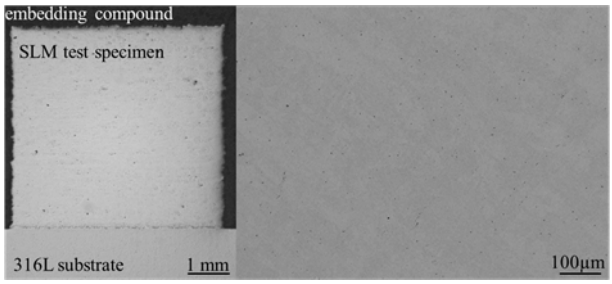

Fig. 1: left: polished cross-section of Fe35Mn SLM test specimen; right: SEM image of polished cross-section.

Fig. 2 shows a photograph of a cellular structure made by SLM out of AZ91 (left) and a light microscope picture of a polished cross-section (right).

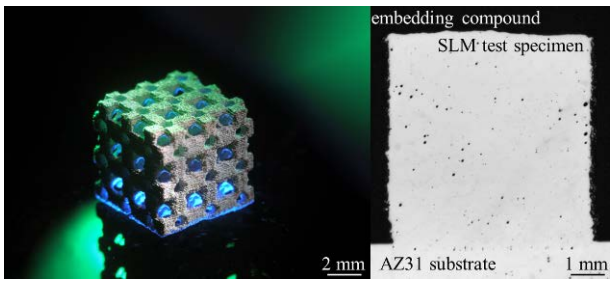

Fig. 2: left: cellular structure out of AZ91; right: polished cross-section of AZ91 SLM test specimen

DISCUSSION & CONCLUSIONS: SLM seems to be a promising manufacturing method for biodegradable metal implants. However, further research is required to determine mechanical and corrosion properties as well as biocompatibility of SLM test specimens out of these materials. Furthermore, the SLM of biodegradable metals has to be adapted to building complex parts such as cellular structures and to other biodegradable iron and magnesium based alloys.

REFERENCES: [1] W. Meiners (1999), *Dissertation RWTH-Aachen University*

ACKNOWLEDGEMENTS: This work was supported by the Fraunhofer Internal Programs under Grant No. MAVO 824682 (DegraLast). The authors thank their colleagues from Fraunhofer IFAM for their help with analyzing Fe35Mn specimens.

Mechanical integrity of magnesium-based biodegradable alloys under combined action of stress and corrosive body fluid

R K Singh Raman[1]
Department of Mechanical and Aerospace Engineering, Department of Chemical Engineering
Monash University (Melbourne), VIC 3800, Australia, [1] raman.singh@monash.edu

BACKGROUND: Addressing health issues of an ageing population is among the greatest challenges of current times. In this regard, use of magnesium (Mg) alloys for temporary implant devices (such as pins, wires, screws, plates, stents etc is emerging as an innovative and extremely attractive approach, since using magnesium alloys will completely avoid the cumbersome procedure of second surgery (which is commonly undertaken to remove such temporary implants when implants are constructed out of commonly used traditional materials (titanium alloys/stainless steels).

Among all metallic engineering materials, magnesium possesses one of the best bio-compatibilities with human physiology, and magnesium alloys also possess the best mechanical compatibility with human bones, besides their required mechanical strength. Use of magnesium alloys as human implants has attracted forefront research attention [1-4]. However, in such use, the alloys must possess adequate resistance to cracking/fracture under the simultaneous action of the corrosive human body fluid (HBF) and the mechanical loading characteristics of human body.

Human-body fluid-assisted fracture has always been among major concerns [5] in use of implants of traditional materials. Recent study on this topic [6] resoundingly establishes such fracture to be among the major concerns, yet vastly underexplored research area in use of Mg alloys as bio-implants. Preliminary studies at the Author's group suggested human-body-fluid-assisted fracture of Mg alloys [7], whereas the subsequent comprehensive studies [8,9] have confirmed such fracture in a traditional Mg alloy (Fig 1).

SCOPE OF PRESENATION: This presentation will first present an overview the mechanical integrity of magnesium alloys under combined action of stress and corrosive body fluid, and then, discuss SCC susceptibility of a few magnesium alloys that have very recently been found to be suitable for temporary implant applications through in-vivo and in-vitro tests. To assess the life of the implant devices that often possess fine micro-cracks, a fracture mechanics based study, i.e. circumferential notch tensile (CNT) testing was performed on notched specimens in physiological environment. CNT tests also generated data for threshold stress intensity factor for stress corrosion cracking (K_{ISCC}). Fracture surfaces of failed specimens have been analysed using scanning electron microscopy.

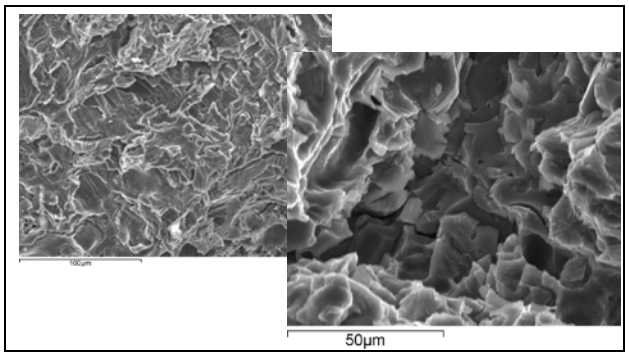

Fig 1: *Trans-granular (top) and Inter-granular fracture of a Mg-alloy in the body fluid, i.e., an evidence of SCC [8]*

REFERENCES:

1. B Zberg, PJ Uggowitzer, JF Löffler (2009) MgZnCa glasses without clinically observable hydrogen evolution for biodegradable implants, *Nature Materials*, **8**: 887.
2. E Ma, J Xu, Biodegradable Alloys (2009): The glass window of opportunities, *Nature Materials*, **8:** 855
3. F Witte et al (2006) In vitro and in-vivo corrosion measurements of Mag alloys. *Biomaterials*, **27:** 1013.
4. MP Staige et al (2006) Mg and its alloys as orthopedic biomaterials: A review, *Biomaterials*, **27**: 1728.
5. M Sivakumar, S Rajeswari S (1992) .. Failures in stainless steel orthopaedic implant devices: pit-induced SCC, *J Mater Sci Lett*, **11:** 1039.
6. RA Antunes, MLC de Oliveria (2012) Corrosion fatigue of biomedical metallic alloys, *Acta Biomater*, **8:** 937.
7. MB Kannan, RK Singh Raman (2008) In-vitro Degradation and mechanical integrity of Calcium-containing magnesium alloys in modified-simulated body fluid, *Biomaterials*, 29 (2008) 2306.
8. L Choudhary, RK Singh Raman (2012) Magnesium alloys as body implants: Fracture mechanism under dynamic and static loadings in a physiological environment, *Acta Biomaterialia*, **8:** 916.
9. MB Kannan, RK Singh Raman (2008) Evaluation of SCC behaviour of AZ91 alloy in modified-simulated body fluid for orthopaedic implant application, *Scripta Mater*, **59:** 175.

Bending strength and crack propagation in cast Mg10Gd influenced by corrosion

P Maier[1], CL Mendis[2], G Tober[1], J Briesemeister[1], E Minciel[1], N Hort[2]

[1] *University of Applied Sciences Stralsund, Stralsund, Germany*

[2] *Magnesium Innovation Centre, Helmholtz-Zentrum Geesthacht, Geesthacht, Germany*

INTRODUCTION: The use of biodegradable implant materials helps to lower the costs and the burden for the patients as the implant removal surgery is avoided. Compared with other degradable materials like polymers, Mg alloys show higher tensile and compressive strength and the young's modulus is closer to that of the cortical bone[1]. However, an implant that is degrading too fast will fail under loading. Alloying with Rare-Earth elements is a promising mechanism to lower the corrosion rate of pure Mg. The best combination of mechanical properties and corrosion rate of the binary Mg-Gd system was found at 10 wt.% Gd[2]. Unfortunately Mg alloys undergo pitting corrosion causing stress corrosion cracking initiation. Pits lead to local increase in the intensity of a stress field and accelerate environmentally induced crack propagation. Implants, like bone screws or nails are exposed to bending, but the influence of corrosion on bending strength has not been investigated.

METHODS: Three-point bending tests were conducted on a TIRA28100 universal testing machine. A span of 90 mm was used for all the plates having a geometry of 110x20x4 mm³. The diameter of the support brackets and plunger were 10 mm and the deformation speed was 1 mm/min.

To investigate the influence of corrosion on the bending strength and crack initiation leading to crack propagation the following approach was used. Three-point bending was conducted on as-cast coarse grained Mg10Gd solution treated (T4: 525 °C for 24 h) to increase elongation at fracture (3.5 %, TYS 68 MPa and UTS 112 MPa) and to reduce the dendritic microstructure:
(a) Mg10Gd (7K)
(b) Mg10Gd pre-corroded (1K, 5K, 8K)
(c) Mg10Gd pre-corroded_bent_corroded (5K)
(d) Mg10Gd pre-bent_corroded (7K).

Ringer-Acetate solution is used in this study due to its proximity to human blood. Plates were corroded for 1 day in 500 ml electrolyte (the pH-level increased to 8.5). The white $Mg(OH)_2$ layer was not removed before bending, however, some parts fall off during the tests.

RESULTS: Fig. 1 shows the influence of pre-corrosion and pre-bending on the retained bending strength. Pre-corrosion reduces the strength by 50 MPa (see 7K and 5K/8K). Corrosion of pre-bent /cracked samples lowers final strength by 30 MPa (7K). Cracking starts at the maximum stress and retained strength is dependent on the crack length. Corrosion after bending/cracking of pre-corroded samples reduces final strength by 22 MPa (5K).

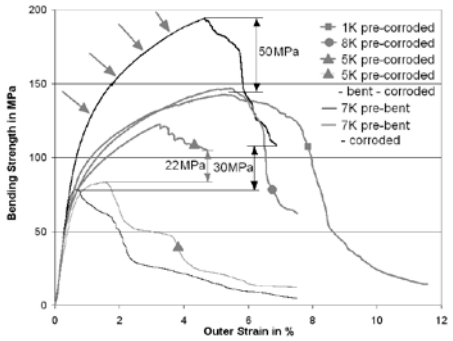

Fig. 1: Bending strength of cast Mg10Gd_T4 influenced by pre-corrosion and pre-bending.

DISCUSSION & CONCLUSIONS: The optical micrograph in Fig. 2 shows the middle section the crack path. The crack propagation is mostly transgranular and interacts with twinning. Double and secondary twinning has also been found.

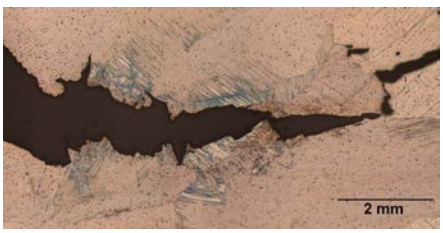

Fig. 2: Crack propagation and twinned grains.

A first approach was done to discuss a) the decrease in bending strength by corrosion and b) to accelerate corrosion by formation of cracks. Now strength loss only by cold work before cracking needs to be investigated (see arrows in Fig. 1 indicating different degrees of deformation).

REFERENCES: [1]M.P. Staiger et al. Biomaterials Vol. 27(9) 2006, 1728-1734. [2]N. Hort et al. Acta Biomaterialia Vol. 6(5) 2010, 1714-1725.

Effects of grain size on the corrosion resistance of Mg-Zn-Ca Alloy

D Liu*, L Liu, Y Liu, R Song, M Chen
School of Materials Science and Engineering, Tianjin University of Technology, Tianjin 300384, People's Republic of China

INTRODUCTION: As well known, grain refine can improve the mechanical strength and ductility of magnesium alloy. However, researches which focus on the effect of grain refine on corrosion resistance of magnesium alloys are still relatively scarce up to now. The objective of present work is to investigate the effect of grain size on the corrosion resistance of Mg-2Zn-0.5Ca alloy.

METHODS: Pure Mg ingot was melted at 720 ºC under the protection of gas mixture containing SF6 and N_2. Calculated amounts of pure Zn and Mg-45%Ca master alloy (Mg–2Zn–0.5Ca, all in wt.%) were added to the Mg melt and then held for 30 minutes to ensure that Zn and Mg-Ca master alloy get melted and diffuse sufficiently. The melt was cast into a wedge shaped copper mould to obtain the Mg–2Zn–0.5Ca alloy with different grain size. The immersion test was performed in the SBF at 37°C by using immersion oscillator. Potentiodynamic polarization and electrochemical impedance spectroscopy (EIS) experiments were performed in a threeelectrode cell, using a Zahner Zennium electrochemical workstation.

RESULTS & DISCUSSION: Fig.1 shows the typical microstructure of the Mg-2Zn-0.5Ca alloy with different grain size .The average grain size is 165um(fig.1(a)) ,120 um(fig.1(b)), 80 um(fig.1(c)), 45 um(fig.1(d)) and 15 um(fig.1(e)), respectively. The polarization curves and electrochemical impedance spectroscopy of the Mg-2Zn-0.5Ca alloy with different grain size indicated that with the decrease of the grain size, the alloy exhibited higher open circuit potentials and larger dimension of capacitance loops , suggesting that the grain refine can decreases the corrosion rate of Mg-2Zn-0.5Ca alloy. Surface morphology of Mg-2Zn-0.5Ca alloy showed that with the grain size decrease, the corrosion production reduced and the homogeneous of corrosion is improved. The possible reasons are as the following: firstly, the uniformity of the chemical constituents and second phase were improved, hence the local micro-galvanic corrosion can be decreased; secondly, the continuity of intergranular eutectic phase are increased as the grain size reduce, which can play as a barrier on the corrosion of magnesium alloy.

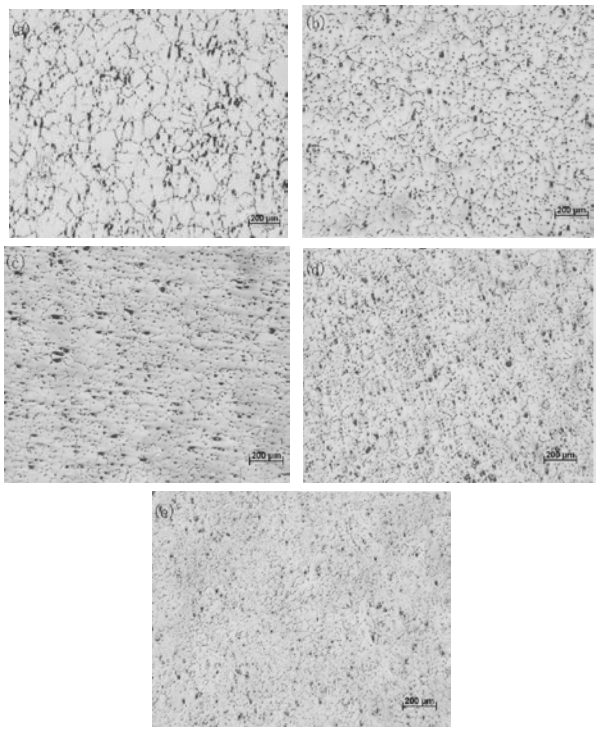

Fig.1 Typical microstructure of the Mg-2Zn-0.5Ca alloy with different grain size: from (a) to (e), the grain size decreases gradually

CONCLUSIONS: With the grain refiner, the resistance and homogeneous of corrosion of Mg-2Zn-0.5Ca alloy were improved, which could been explained from point of view of microstructure changes: (1) the uniformity of the chemical constituents and second phase are improved. (2) the distributes continuity of intergranular eutectic phase are increased.

REFERENCES:

[1] *M.P. Staiger, A.M. Pietak, J. Huadmai, G. Dias, Biomaterials 27 (2006) 1728-1734*

[2] *Frank Witte, Acta Biomaterialia 6 (2010) 1680–1692*

ACKNOWLEDGEMENTS: Acknowledgements The authors are grateful for the supports from the National Natural Science Foundation of China (No. 51271131).

Biodegradation behaviour of magnesium alloy under flow-induced shear stress

J Wang[1.2], V Shanov[3], ZG Xu[1], Y Jang[1], V Giri[1], B Collins[1], J Sankar[1], N Huang[2],Y Yun[1]

[1] Engineering Research Center for Revolutionizing Metallic Biomaterials, North Carolina A & T State University, NC,USA. [2] Key Lab. of Advanced Materials Technology, Ministry of Education, Southwest Jiaotong University, China. [3] College of Engineering, University of Cincinnati, OH, USA. Email: yyun@ncat.edu (Y. Yun)

INTRODUCTION: Mg-based metals have promising potential as biodegradable implants in vascular applications, such as carotid artery, cerebral artery, coronary artery, femur artery, ureter, etc. Although their biodegradation is a complex multifactorial process in these implanting positions, flow-induced shear stress (FISS) has emerged as an essential feature of degradation behaviour [1]. The purpose of this study is to explore various corrosion types, corrosion rate, composition and amount of corrosion products, and hydrogen cracking under different values of FISS. Understanding corrosion behaviour is critical since it is further related to biocompatibility or toxicity.

METHODS: A vascular bioreactor was developed and FISS was varied at 0, 0.3, 0.6, 1.2 and 2.3 Pa for a MgCaZn alloy and 0 and 0.25 Pa for a AZ31B stent, which were calculated by fluidic flow simulation (COMSOL). The samples were incubated in 200 ml of DMEM with 10% Fetal Bovini Serum and 1% Penicillin-Streptomycin under cell culture conditions (37 °C, 5% CO_2 and 95% rH) and peristaltic pump was used to flow the solution. After corrosion tests, samples were extracted and analyzed by X-ray computed tomography. The 2D planes and 3D models were reconstructed using a phoenix datos|x software. Corrosion morphologies and the composition and thickness of corrosion products were characterized by SEM and EDX.

RESULTS & DISCUSSION: With the increasing of FISS, more localized corrosions and higher corrosion rate were observed, and corrosion products were washed away at higher FISS (Fig. 1 dark regions). In the uniform corrosion regions, the thicknesses of magnesium hydroxide were increased with the increased FISS, but that of CaP complex did not show significant change (Fig. 2a). Metal penetration can be expressed in terms of a pitting factor [2], as shown in the following relationship:

Pitting Factor = deepest metal penetration / average metal penetration, which is the ratio of maximum depth of local corrosion to the thickness of uniform corrosion layer (Fig. 2b). Pitting factors under 0, 0.3, 0.6, 1.2 and 2.3 Pa in FISS were 19.6, 45.0, 54.7, 56.4 and 52.2, respectively. In AZ31B stent degradation test (Fig.3), the thickness of corrosion products in dynamic test (FISS: 0.25Pa) was thicker than that in static test. Corrosion type under static condition mainly displayed localized corrosion (green frame), however corrosion type under dynamic condition was more uniform corrosion with some exfoliations facing the direction of flow (yellow frames).

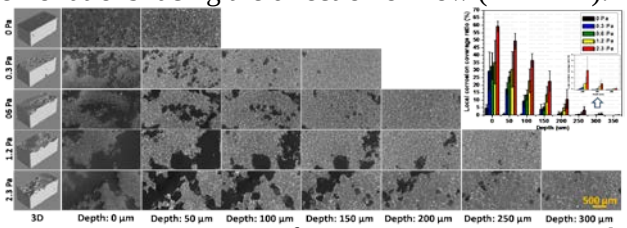

Fig.1. Reconstructions of X-ray Micro-CT 3D with different depth 2D slices of samples under different values of FISS. Localized corrosion coverage ratios under different depths were calculated from CT data.

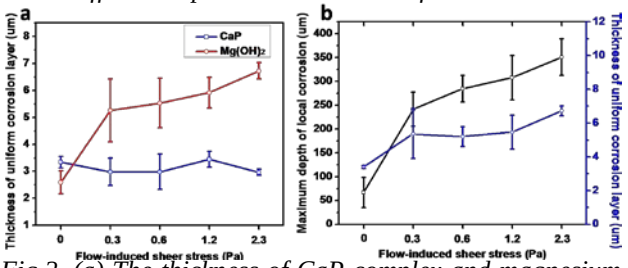

Fig.2. (a) The thickness of CaP complex and magnesium hydroxide on the uniform corrosion region. (b) The maximum depth of localized corrosion and uniform corrosion layer from Micro-CT and EDX analysis.

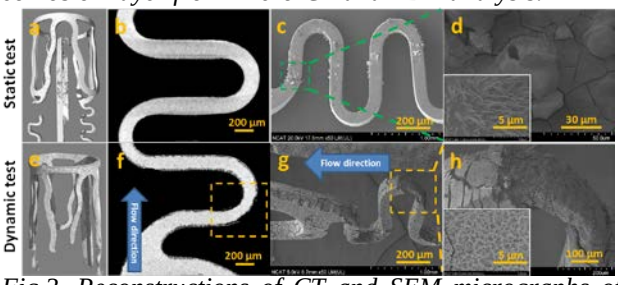

Fig.3. Reconstructions of CT and SEM micrographs of stents under static and dynamic degradation condition.

CONCLUSIONS: Understanding biodegradation behaviour of Mg alloys under FISS can lend insight into biocorrosion mechanism in vivo, and provide support for expanding clinic applications of Mg-based stents in multifarious implanting positions.

REFERENCES: [1] J. Levesque, H. Hermawan, D. Dube, et al (2008) *Acta Biomater* **4**:284–295. [2] ASTM Standard Guide (2005) G46-94.

ACKNOWLEDGEMENTS: NSF-funded ERC for RMB (0812348), PhD Innovation Fund of SWJTU (2011) and China Scholarship Council (201207000016).

Investigation of coated magnesium alloys by IR, Raman, X-ray and Mass spectrometry

K Vano-Herrera[1], F Zimmermann[1], M Stekker[2], C Vogt[1]

[1] *Leibniz University Hannover, Institute for Inorganic Chemistry, Germany.* [2] *MeKo, Sarstedt, Germany*

INTRODUCTION: Polymer coated alloys are increasingly used to change the starting conditions for *in vivo* corrosion or/and to apply anti-inflammatory or immune response suppressing drugs during the dissolution or degradation of the coating system. While corrosion behaviour of uncoated alloys was investigated in detail during the last years, less is known about the impact of the protecting polymer layers on the corrosion and the degradation of the polymers or the drug release *in vitro* and *in vivo*.

METHODS: IR and Raman microscopy as well as mass spectrometric techniques have been used to obtain information about coating polymers, their degradation products and released drugs, although quantification within the often only 10 µm thin layers is challenging. In parallel degradation products of the coated alloys were measured by X-ray and mass spectrometric techniques and background values for the alloying components in different biomatrices were determined by mass spectrometry.

RESULTS & DISCUSSION: For quantification of polymers in protecting layers by IR or Raman spectroscopy synthesis and preparation of reference standards was crucial as well as selection of best conditions to discriminate between the polymers or drugs and the surrounding biomatrix. The presentation will show this procedure exemplarily for a coated magnesium stent.

The determination of corrosion products for the alloying components was performed by PIXE measurements. Influence of polymer layer and position of implantation on the degradation have been determined by measuring the concentrations of all alloy components in the degrading alloy as well as the surrounding biomatrix.

Background values in liver, kidney, bone or muscle for most of the alloying components in magnesium alloys (REE, Zn, Ag, Al, Li, and others) are in the ppb (µg/kg) or sub-ppb level (Table 1). Special sample treatment and working under clean room conditions was necessary to determine these concentrations in rat and rabbit and to allow for decisions whether enrichments of alloying components takes place in organs of living species after degradation of the alloy.

Table 1. Background concentration for selected alloying components in liver and bone of New Zealand White Rabbit.

Element	Liver	Bone
Mg	170-210 mg/kg	0.20-0.25 %
Zn	30-40 mg/kg	110-170 mg/kg
Al	40 µg/kg	190 µg/kg
Li	1.4 µg/kg	80 µg/kg
REE	0.3-3 µg/kg	

REFERENCES: [1]S. Gruhl, F. Witte, J. Vogt, C. Vogt (2009) *JAAS* **24**: 181-188. [2] C. Vogt et al (2009) Investigation of the degradation of biodegradable Mg implant alloys *in vitro* and *in vivo* by analytical methods in *Magnesium* (ed. K.U. Kainer) Wiley-VCH, pp 1162-1174.

ACKNOWLEDGEMENTS: We like to acknowledge the support of this work by Prof. F. Witte by providing animal samples for the determination of background values.

Electrochemical detection of magnesium ions using magnesium biosensor

S Natasha, RSP Malon, DHB Wicaksono, EP Córcoles, H Hermawan

Faculty of Biosciences and Medical Engineering, Universiti Teknologi Malaysia (UTM), Malaysia

INTRODUCTION: Electrochemical enzymatic biosensors are recognized for their sensitivity, selectivity and temporal resolution. This biosensor can potentially be used to monitor the degradation of biodegradable metals such as magnesium (Mg) in real-time and *in vivo*, which cannot be done by common imaging techniques (X-ray, CT, etc.). The biosensor fabrication is based on the requirement of Mg ions during kinase enzymatic reactions, which provides the required selectivity to the technique [1]. This work aims to develop a biosensor system to measure the concentration of Mg^{2+} ions released during the Mg degradation.

METHODS: Cotton cloth (Mirota Batik, Indonesia) was used as an immobilization platform to fabricate the biosensor, namely cloth analytical device (CAD), by using simple assembly techniques described elsewhere [2]. The CAD was comprised of a hydrophilic reaction zone delimited by a hydrophobic area. Three electrodes were embedded on the reaction zone: working and counter electrodes using carbon-Prussian Blue paste and a reference electrode using Ag/AgCl paste (Gwent Electronics Material, England). 3 µl of enzyme mix solution (20 mg/ml, 1:1, Glycerol Kinase (GK) and Glycerol-3-Phosphate Oxidase (GPOx)) were entrapped within the cellulose fibers. A glycerol buffer solution (3 mM of adenosine triphosphate (ATP) and 500 µM glycerol in 0.1 M PBS) was used to prepare Mg^{2+} standards (5 - 1000 µM) as glycerol was the substrate of the enzymatic reaction. 3 µl of Mg^{2+} standards were pipetted onto the reaction zone and the current obtained with both cyclic voltametry and chrono-amperometry techniques was detected using a µSTAT400 potentiostat (DropSens, Spain).

RESULTS: Figure 1 shows cyclic voltammetry curves of Mg^{2+} standards where the measurement was performed in a range of -0.5 to +0.5 V at a scan rate of 10 mV/s. The optimum catalytic reduction of H_2O_2 in the electrodes occurred at -0.2 V. Hence, this working potential was selected for chrono-amperometric measurements.

The CAD was capable of detecting concentrations of Mg^{2+} up to 1000 µM (Fig. 1 inset) and showed a good repeatability or reproducibility (relative STDEV = 13.50%, n = 3).

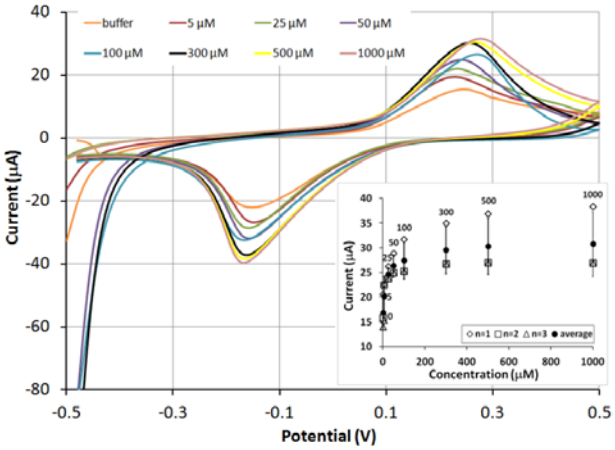

Fig. 1: Cyclic voltametry of Mg^{2+} standards. Mg^{2+} calibration curve shows current plotted versus different concentration of Mg^{2+} ions (inset). Data points are the mean and error bars are the STDEV of the mean (n=3).

DISCUSSION & CONCLUSIONS: The detection of the CAD ranges from 5 to 1000 µM with sensitivity, determined from the slope of the linear calibration curve at 5-100 µM, of 0.001 µA/µM (Fig. 1). The limit of detection, determined as 3 x STDEV, was 10.16 µM. These showed an improvement when compared with common colorimetric assay kits, where the sensitivity ranges from 6 to 300 µM with detection sensitivity of 40 µM [3]. Since the concentration of Mg^{2+} in blood serum is commonly 0.7-1.05 mM (1.65-2.55 mg/dl) and the upper and lower limit are 3 and 9 nmol, respectively [3], the developed CAD will have the capability of detecting the Mg concentration in the serum. Although further studies are necessary to test the interference species and to improve the reproducibility of the device, the CAD has the potential to be implanted *in vivo* during surgery to monitor the corrosion rate of biodegradable Mg implants.

REFERENCES: [1] M.E. Ghica and C.M.A. Brett (2006) *Anal Lett* **39**: 1527-42. [2] A. Nilghaz, D.H.B. Wicaksono, D. Gustiono, et al (2012) *Lab Chip*, **12**:209-18. [3] BioVision (2013) Mg-Colorimetric Assay Kit: http://www.biovision.com.

ACKNOWLEDGEMENTS: Malaysian Ministry of Higher Education and UTM (ERGS R.J130000.7836.4L019).

Effect of stress on the corrosion behaviour of magnesium wire in m-SBF

S Zhang [1], X Li[2], H Wu[2], C Zhao[2], J Liu[1], Y Zhang[1], X Zhang[1,2]

[1]Suzhou Origin Medical Technology Co., Ltd. [2]School of Materials Science and Engineering, Shanghai Jiao Tong University

INTRODUCTION: Due to the biodegradation property and good biocompatibilities, magnesium alloys have been worldwide investigated as bone fixation materials or vascular intervention devices. Magnesium wire can also be used as preferable biodegradable materials for surgical applications[1], for example, linear cuter staples, suture wires or other surgical closing devices or tracheal stents. In the present study, pure magnesium wire was fabricated and then the degradation behaviours under different stress levels were researched.

METHODS: High purity magnesium wire with a diameter of 0.3mm was fabricated (Fig.1a), which was cut into 10cm long for immersion tests. The degradation tests were done in a device shown in Fig.1b. The sealed container is a burette and so the hydrogen evolution can be observed. Fracture time points of the wire are also recorded.

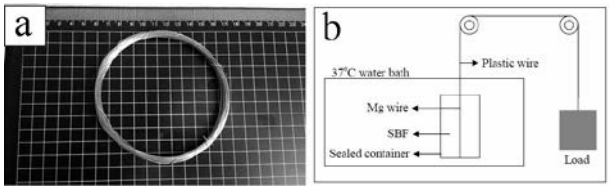

Fig.1a: High purity Mg wire used in the present study; Fig.1b: Illustration of wire degradation setup in different stress levels, in which different stress levels are provided by different loads

RESULTS: Fig.2a and Fig.2b are the hydrogen evolution results and breaking times under different stress levels, respectively. According to Fig.2, it can be observed that the stress levels strongly affect the degradation behaviour of Mg wire. When the stress is increased, the hydrogen evolution rate became faster, and the wire fractured earlier under a higher stress level. Especially when the stress level is increased from 0 to 20MPa, the fracture time is undermined from 550h to nearly 240h (10 days, a critical time point of stomach or intestine curing period), i.e. nearly a half life of the wire was reduced.

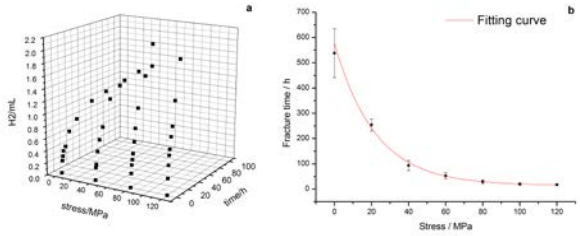

Fig.2a: Hydrogen evolution results of Mg wire during immersion. Fig.2b: Fracture time points versus different stress levels.

DISCUSSION & CONCLUSIONS: Magnesium wire can be widely used in current clinics, especially for linear cuter stapler or other closing devices made of wires. While the present closing devices (e.g. staples) are made of titanium alloys, which are permanent and will stay in the human body forever. As a result, certain complications such as inflammation may occur in long term. And due to the absorption of X-Ray caused by titanium, future CT results may also be affected by the residual devices. Therefore the degradable magnesium wire is a promising substitute. However, after use these devices will bear stress. For example, the staple nail is U-shape and after use it becomes B-shape, therefore severe deformation and residual stress are obvious. In addition, the tissue (such as stomach or intestine) may impose pressure on the devices. So the degradation behaviours under stresses are quite important for Mg wire. According to the results of the present study, it should adjust the detailed parameters of the closing devices to avoid that high residual stress after deformation will not be above a critical level, for example, 20MPa. Otherwise the life of the closing devices nail may not meet the requirements of cure.

REFERENCES: [1]AC. Hazi et.al.(2011) *Materials Science and Engineering C.31:1098–1103.*

ACKNOWLEDGEMENTS: The authors are grateful for the supports by the Jiangsu Nature Science Foundation for Young Scholars (Grant No. BK2012206) and the Nature Science Fundation (Grant No.51271117) of China.

Nanorod-shaped hydroxyapatite formed on pure magnesium by Micro-arc oxidation and hydrothermal treatment

B Li[1], Y Han[1]

[1.] *State-key Lab for Mechanical Behavior of Materials, Xi'an Jiaotong University, Xi'an 710049 China*
Email: yonghan@mail.xjtu.edu.cn

INTRODUCTION: Magnesium (Mg) and its alloys have shown great potentials for orthopedic implants However, their high degradation rates in physiological environment and consequent loss in the mechanical integrity could limit their clinical application. Many efforts have been done to control the degradation, surface modification especially the Micro-arc oxidation (MAO) [1] coating have shown to be an effective way in enhancing their corrosion resistance and keeping mechanical integrities before the tissues sufficiently heal. However, the micropores in the MAO coating can be the channels between the corrosion medium and substrate and reduce the corrosion resistance. Besides improving the biodegradation rate, the biocompatibility should also be considered. So in this work, a novel coating composed of nanorod-shaped hydroxyapatite (HA) and dense MgO bilayers with high bond strength was formed on Mg, and the corrosion resistance of the bilayers coated Mg was also investigated.

METHODS: To form MgO coating, micro-arc oxidation (MAO) of Mg was performed in an aqueous electrolyte using a pulse power supply at a fixed applied voltage for 10min.The as-MAOed Mg samples were subsequently mounted into a Teflon-lined autoclave with an aqueous solution containing 0.25 M $C_{10}H_{12}CaN_2Na_2O_8$ (Ca-EDTA) and 0.25 M K_2HPO_4, and the PH was adjusted to 9 with NaOH solution to receive hydrothermal treatment (HT) for 0.5, 1, 5 and 12 hours, respectively. The phase components, morphologies and elemental compositions of the coatings were examined by XRD and FESEM. Polarization test of the coatings coated Mg samples were carried out in physiological saline at 37℃ with the application of Autolab potentiostat.

RESULTS & CONCLUSIONS: Fig 1 shows the surface changes of as-MAOed coating after HT for different time. After HT for 5h (Fig 1(c)), the dense nano-rodshaped HA with the diameter of 80nm and length of 800nm which was confirmed by XRD pattern in Fig 1(e) was synthesized on the as-MAOed coating. From the cross-section view (Fig 1(d)) the micropores produced by MAO process were sealed with nanorod-shaped HA formed during HT, which can be acted as a barrier to prevent the corrosion solution permeate into the pores and corrode the substrate directly. This assumes was confirmed by the polarization test (Fig 1(f)), the corrosion current of the pure Mg, as-MAOed and MAO+HT5h was 1.513×10^{-3}, 4.06×10^{-6} and 2.8×10^{-8}, respectively. After HT, the corrosion resistance of MAO+HT coating was enhanced compared with the as-MAOed sample.

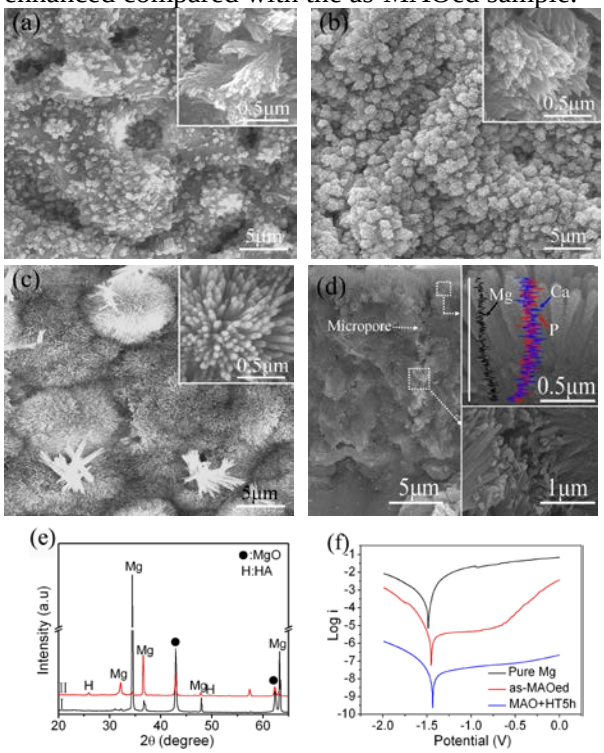

Fig 1: Surface morphologies of the as-MAOed coating, and the coatings subjected to HT for (a) 0.5, (b) 1h and (c) 5h; (d) cross-sectional morphologies of 5 h HTed MAOed-coating for; (e) XRD patterns of the MAOed Mg before (I) and after HT for (II) 5h; (f) Potentiodynamic polarization curves of pure Mg, as-MAOed and HT for 5h.

REFERENCES: X.N. Gu, N.Li, W.R. Zhou, Y.F. Zheng, X. Zhao, Q.Z. Cai, Liquan Ruan, *Acta Biomaterialia* 7 (2011), 1880-1889

Inhibitor-loaded chitosan coatings on the microarc oxidized Mg-1Ca alloy

ZJ Jia[1], M Li[1], Q Liu[1], XC Xu[1], Y Cheng[1,*], YF Zheng[1,2], TF Xi[1], SC Wei [1,3]

[1]*Center for Biomedical Materials and Tissue Engineering, Academy for Advanced Interdisciplinary Studies, Peking University, PCR* [2]*Department of Advanced Materials and Nanotechnology, College of Engineering, Peking University, PCR* [3]*Department of Oral and Maxillofacial Surgery, School and Hospital of Stomatology, Peking University, PCR*

INTRODUCTION: The medical application of the promising biodegradable Mg-Ca alloy is hindered by its mismatched fast corrosion rate with the tissue healing rate[1]. A new corrosion prevention strategy based on self-healing characteristic of "green" chitosan was proposed[2]. Cerium compounds were efficient in corrosion inhibiting of Mg alloys[3]. Microarc oxidation (MAO) is known for the excellent substrate adhesion of the resultant porous coating. In this study, MAO combined with dip coating were utilized to fabricate a Ce-loaded MAO/CS hybrid coating on Mg-1Ca alloy to improve its corrosion resistance.

METHODS: The cubic Mg-1Ca (wt.%) plates (extruded, 10×10×2 mm^3) were used. The MAO process was performed in an alkaline KF-silicate electrolyte under 360 V for 10 min, followed by a 15 min-dipping in 1 wt.% $Ce(NO_3)_3$-containing chitosan (CS-Ce) solution. The chitosan solution was prepared by dissolving the as-received chitosan (MW=20×10^4, DD=85%) at one weight percentage in 0.2% acetic acid. The coating morphologies and composition were investigated by SEM and XPS/XRD, respectively. Electrochemical tests were carried out to evaluate their corrosion resistance in Kokubo's SBF solution.

RESULTS: The Ce-loaded MAO/chitosan hybrid coating was developed on Mg-1Ca alloy. The 20 μm thick MAO pre-layer had a ceramic-like porous structure (*Fig. 2B*), and it was composed of MgO, MgF_2 and Mg_2SiO_4 (not shown). SEM depicted the hybridization of CS-Ce top-layer with the MAO pre-layer via sealing/bonding effect (*Fig. 2A*). XPS and FTIR results confirmed the successful loading of cerium by interaction with chitosan (*Fig.* 1). Electrochemical tests demonstrated significant decrease in current density (I_{corr}) and obvious enhanced AC impedance properties (*Fig. 2*) of the hybrid coating in SBF.

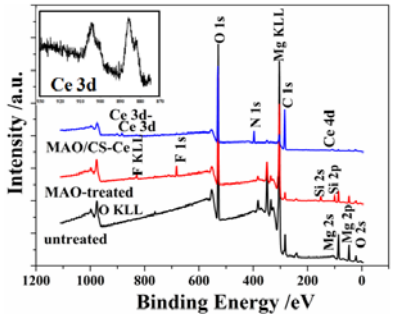

Fig. 1: XPS spectra of untreated, MAO-treated and MAO/CS-Ce treated Mg-1Ca samples

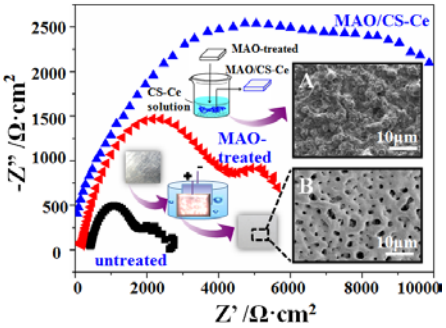

Fig. 2 Nyquist plots for different samples obtained in SBF after 1 h stabilization

DISCUSSION & CONCLUSIONS: The MAO pre-layer enabled good substrate adhesion and served as intermedia for the deposition of CS-Ce chitosan coating. The sustainable release of inhibitor cerium ions provided long-term active prevention of Mg-1Ca.

REFERENCES: [1] Z.J. Li, X.N. Gu, S.Q. Lou, et al (2008) *Biomateirals* **29**:1329-44. [2] M.L. Zheludkevich, J. Tedim, C. S. R. Freire, et al (2011) *J Mater Chem* **21**:4805-12. [3] M. Dabala, K. Brunelli, E. Napolitani, et al (2003) Surf Coat Technol **172**: 227-32.

ACKNOWLEDGEMENTS: This work was supported by National Natural Science Foundation of China (No. 31070846 and 30870623), National High Technology Research and Development Program of China (No. 2011AA030103), and National Basic Research Program (973) of China (No. 2009CB930004 and 2012CB619102).

In vitro biocorrosion behavior of NZ20K alloy evaluated by different methods

X Zhang[1], G Yuan[2], Z Wang[1], Y Xue[1]

[1] School of Materials Science and Engineering, Nanjing Institute of Technology, China. [2] National Engineering Research Center of Light Alloy Net Forming, Shanghai Jiao Tong University, China

INTRODUCTION: Mg-Nd-Zn-Zr alloy is a promising biodegradable magnesium alloy for biomedical applications due to its high strength, high corrosion resistance and acceptable cell toxicity [1-2]. For the limited resource, the price of rare earth elements Nd rises recently. In this study, Mg-2.25Nd-0.11Zn-0.43Zr (wt.%, NZ20K) was prepared to reduce the Nd addition. Three methods were conducted to evaluate *in vitro* biocorrosion behavior of the alloy.

METHODS: The cast ingot of NZ20K alloy was solution treated (T4). The ingot at T4 state was hot extruded into rods (E), and then, were aged (EA). Microstructure was observed by scanning electron microscopy (SEM). The immersion tests, including mass loss test (ML) and hydrogen evolution test (HE), prolonged for 120 h in simulated body fluid (SBF), and the electrochemical polarization test (EP) was conducted after immersion in SBF for 1h. The details of the biocorrosion tests can be referred to Ref [1]. The biocorrosion results of the HE and EP were also converted into mm/year and compared with those obtained by ML. All the tests were triplicated.

RESULTS: The grain is significantly refined by extrusion. Aging treatment on E alloy shows no obvious difference in microstructure. The SEM images of T4 and EA alloy are shown in Fig. 1. Large number of pits can be observed from T4, and some bright particles can be seen. The bright particles are Zr-rich compound, and lots of them peeled off during etching the microstructure, resulted in the pits.

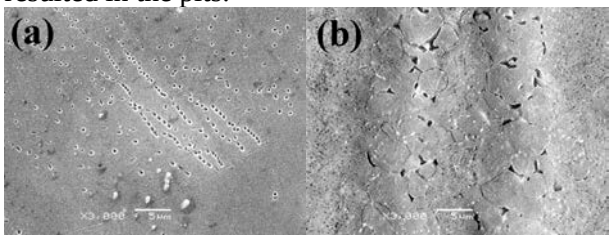

Fig.1 Images of the NZ20K alloy (a) T4 and (b) EA

The biocorrosion rates of the alloy obtained by ML, HE and EP experiments are listed in Table 1. The results by different tests show the same tendency that the biocorrosion rate of the alloy follows the order EA<E<T4 (except EP results of EA) but different values. Generally, the values obtained by ML are the highest, while those obtained by EP are the lowest. Moreover, the T4 results show the most deviation among the alloy under three conditions obtained by three methods.

Table 1. In vitro biocorrosion rates of the NZ20K alloy obtained by three methods

Sample	Biocorrosion rate (mm/year)		
	ML	HE	EP
T4	0.35±0.04	0.20±0.01	0.14±0.02
E	0.27±0.06	0.18±0.03	0.12±0.01
E A	0.21±0.03	0.16±0.04	0.13±0.05

DISCUSSION & CONCLUSIONS: Lots of pits, which were not undergone corrosion but caused during removing corrosion products by acid solution, formed on the surface of T4 (Fig. 2a). However, few such pits can be observed in EA (Fig. 2 b). Therefore, the deviation of T4 by ML and HE is more significant than that of EA. The EP values, which are the lowest, are probably attributed to the formation of a protective layer on the surface of the alloy at the early stage because it doesn't reflect the changing nature of corrosion rate with time [3]. The grain refinement and precipitation are responsible for the improvement of the corrosion resistance of E and EA.

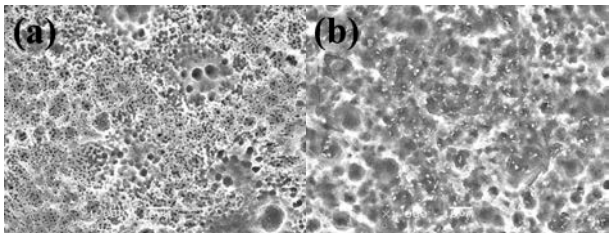

Fig.2 SEM images of the NZ20K alloy after removing corrosion products (a) T4 and (b) EA

REFERENCES: [1] X. Zhang, Z. Wang, G. Yuan, et al (2012) *Mater Sci Eng B* **177**:1113-9. [2] X Zhang, G Yuan, J Niu, et al (2012) *J Mech Behav Biomed Mater* **9**:153-62. [3] N. Kirkland, N. Birbilis, M. Staiger (2012) *Acta Biomater* **8**:925-36.

ACKNOWLEDGEMENTS: This work was supported by the Innovative Foundation Project of Nanjing Institute of Technology (CKJA201201).

Corrosion behaviour of Mg-aCa-bY extrusions in simulated body fluid

CD Yim[1,2], SK Woo[2], YM Kim[1], BS You[1,2]

[1] *Light Metal Division, Korea Institute of Materials Science, Korea.* [2] *School of Advanced Materials Science and Engineering, University of Science and Technology, Korea*

INTRODUCTION: Magnesium alloys have many advantages as biodegradable metals including lightweight, similar elastic modulus to bone and non-toxicity. But there are some barriers such as poor corrosion resistance and low absolute strength to be overcome for wide applications of magnesium alloys as biodegradable implants and stents. In this study, the effects of complex addition of Ca and Y on corrosion behavior of magnesium were evaluated by immersion and potentiodynamic tests in simulated body fluid (SBF).

METHODS: Mg-based extrusions containing different amount of Ca and Y were produced by indirect extrusion of permanent mold casting billets. Immersion test was carried out in SBF at 310K for 72hours and average corrosion rate was calculated by measurement of weight loss before and after immersion test. Potentiodynamic test was also carried out in SBF at 310K. The open circuit potential (OCP) was measured for 3600s and then the applied potential was changed from -0.25V to +0.5V referred to OCP at scan rate of 0.5mV/s.

RESULTS: Figure 1 shows the average corrosion rates of as-extruded Mg-aCa-bY alloys calculated by weight loss after immersion test.

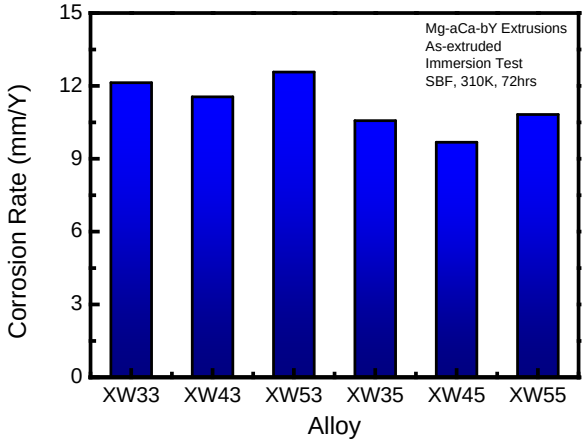

Fig. 1: Average corrosion rates of as-extruded Mg-aCa-bY alloys.

The corrosion rates of extrusions containing 0.5wt.% Y are slower than those of extrusions containing 0.3wt.% Y, which means that Y is effective to improve the corrosion resistance. The corrosion rates of extrusions containing 0.4wt.% Ca are the lowest regardless of the amount of Y. It means that the optimum amount of Ca exists for improvement of corrosion resistance, which is well agreed with the previous studies [1-3].

Figure 2 shows the potentiodynamic curves of as-extruded Mg-aCa-bY alloys. The passivation is observed in anodic polarization region. The passivation may be resulted from formation of protective layer consisted of $Ca_{10}(PO_4)_6(OH)_2$. The current densities in cathodic polarization region increase similarly to increase of average corrosion rate according to the alloy composition.

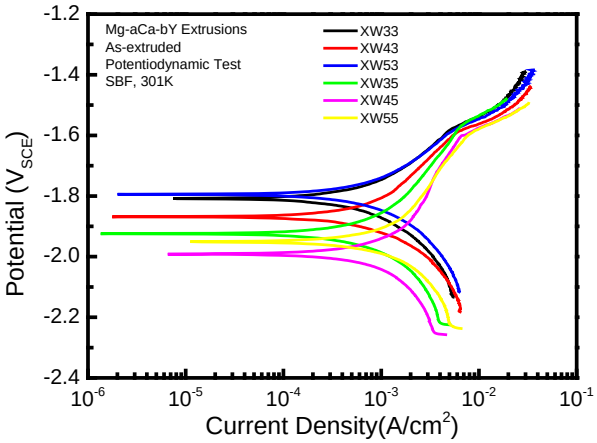

Fig. 2: Potentiodynamic curves of as-extruded Mg-aCa-bY alloys.

DISCUSSION & CONCLUSIONS: The average corrosion rates and the current densities change similarly with alloy composition, which means that the overall corrosion behavior of Mg-aCa-bY is strongly dependent on hydrogen evolution.

REFERENCES: [1] Y. Fan, G. Wu, H. Gao, and C. Zhai (2006) *J. Elecrochem Soc* **153**:B283-B288. [2] C.D. Yim, Y.M. Kim, and B.S. You (2007) *Mater Trans* **48**:1023-28. [3] Y.-Q. Wang, M.-Z. Li, C. Li, X.-Y. Li, L.-Q. Fan, T. Jia (2011) *Mater Corr* **63**:497-504.

ACKNOWLEDGEMENTS: This study was financially supported by Korea Institute of Materials Science.

Absorbable Mg-ND composite and Zn alloy for surgical implant application

J Zhou[1], H Gong[1], D Yao[2]

[1] *Mechanical Engineering and Mechanics Department, Drexel University, USA,* [2] *School of Materials Science and Engineering, Georgia Institute of Technology, USA*

INTRODUCTION: Magnesium (Mg) alloy corrodes too fast and quickly loses its mechanical support as implant device. Nano-diamond (ND) particles were introduced to reduce Mg's bulk corrosion rate. On the other hand, Zinc (Zn) based alloy was developed to solve the fast-corrosion problem of metal implants.

METHODS: Mg powder (diameter<50um, purity > 99.8%, Alfa Aesar, USA) was uniformly mixed with ND particles (diameter<10nm, Zhonglian Nanotech, China) in ball mill. The mixture was cold compacted at the pressure of 500MPa, and sintered at 600°C under argon protection. To prepare Zn-1%Mg alloy, pure Zn (99.99%) was melted in a resistance furnace and Mg chips (99.9%) were dipped in. The melt was casted in graphite mold to form rod specimen.

Immersion test was performed according to ASTM-G31-72. Simulated body fluid (SBF) was added by the surface area to solution volume to 1 cm^2:20 ml and temperature was kept at 37 °C. The electrochemical testing circuit was composted of Mg as working electrode, saturated calomel electrode (SCE) as reference electrode and a platinum electrode as counter electrode. The open circuit potential (OCP) was measured for 60mins and the frequency span was set as 100mHz to 100kHz at OCP values with a sinusoidal 10~10mV for potential electrochemical impedance spectroscopy (PEIS) measurement.

RESULTS: Immersion test found out that corrosion rate of fabricated Mg-ND composite was significantly reduced compared to pure Mg, possibly due to the ion-attracting ability and electrical insulating property of ND (Fig.1.A). It was found that ND with functional groups effectively attracted calcium, phosphate, hydroxyl, sulfate and other ions from Simulated Body Fluid (SBF). Along with Mg immersion, ions continuously attached on Mg surface and formed protection layer against corrosion. Mg-ND composite were found to have higher electrochemical impedance than pure Mg, probably due to near-zero electrical conductance of ND particles mixed in Mg matrix (Fig.1.B).

Zn-1Mg alloy corroded at a much lower rate compared with Mg alloy WE43, which is one of the best candidate material for absorbable implant (Tab.1). Electrochemical test found out that Zn is less electrochemically active because corrosion potential of Zn alloy is much nobler than Mg alloy, and electrochemical impedance of Zn alloy is much higher than Mg alloy. Corrosion morphology of Zn-1Mg was shown in Fig.1.C&D.

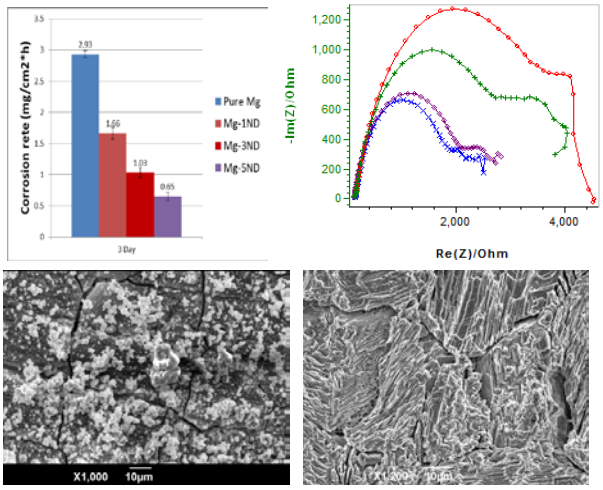

*Fig. 1:A) Corrosion rate of Mg was reduced from 2.93 to 0.65 mg/cm^2*h by adding 5% ND, B) PEIS of pure Mg (blue Diag cross), Mg-1%ND (purple circle), Mg-3%ND (green cross), Mg-5%ND (red circle), C) Corrosion products on Zn-1Mg, D) Morphology of Zn-1Mg after acid washing*

*Tab 1. Comparison of corrosion rates (mg/cm^2*h)*

	2 weeks	4 weeks
Zn-1Mg	0.014	0.0058
WE43	0.038	0.028

DISCUSSION & CONCLUSIONS: Two novel absorbable metal materials, Mg-ND and Zn alloy, have been successfully prepared and characterized. Both materials showed reduced bulk corrosion rate compared with Mg alloy, thus they may be promising candidate materials for absorbable implants.

Hydroxyapatite and octacalcium phosphate coating of bioabsorbable Mg-Ca alloys by a novel chemical solution deposition method

S Hiromoto[1], K Hanada[2] and K Matsuzaki[2]

[1] *Biomaterials Unit, National Institute for Materials Science (NIMS), Tsukuba, Japan.* [2] *Advanced Manufacturing Research Institute, National Institute of Advanced Industrial Science and Technology (AIST), Tsukuba, Japan*

INTRODUCTION: Surface modification is a useful means to control the corrosion and to improve the biocompatibility of bioabsorbable magnesium alloys simultaneously. We developed hydroxyapatite (HAp) and octacalcium phosphate (OCP) coatings with a novel chemical solution deposition and revealed that HAp-coated pure Mg and Mg-3Al-1Zn (AZ31) alloy showed high corrosion resistance in a simulated body fluid and that the HAp coating showed good adhesiveness to the substrate under cyclic loading [1-4]. Mg-Ca alloys were developed as a bioabsorbable metal showing a good strength and ductility balance. In this study, HAp and OCP coatings of Mg-Ca alloys were performed with the chemical solution deposition method.

METHODS: Disks (16 mm^{ϕ} x 2 mm^{t}) were cut from Mg-xCa (x=0.2, 0.4, 0.8 and 1.0wt%) extrusion rods. Disks were polished with #1200 SiC paper and then immersed in a calcium phosphate treatment solution with pH 8.9 at 363 K for 1 hour. The surface was characterized using an X-ray diffraction (XRD) and a backscattered electron microscope (BSEM).

HAp-coated Mg-0.2%Ca and Mg-0.8%Ca alloys were immersed in a simulated body fluid (SBF) only with inorganic chemicals at 310 K for 1day. #1200-polished alloys were used as a reference.

RESULTS: XRD analysis revealed that HAp was formed at pH 8.9 regardless of Ca content of the alloys.

Figure 1 shows surface SEM images of Mg-0.2%Ca alloy treated at pH 8.9. Rod-shape crystals of HAp densely and uniformly covered the surface. The surface micromorphology of HAp coating did not depend on the Ca content.

Figure 2 shows appearance of as-polished and HAp-coated Mg-0.2%Ca alloy immersed in the SBF for 1 day. While the as-polished alloys showed filiform corrosion, the HAp-coated alloys showed small pits mainly and small filiform corrosion rarely.

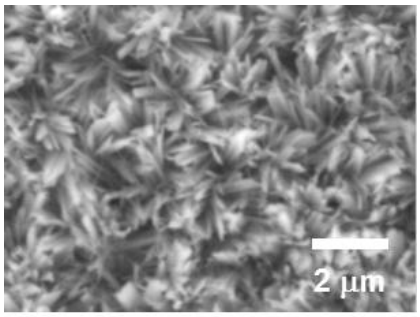

Fig. 1: Surface SEM image of Mg-0.2wt%Ca alloy treated at pH 8.9.

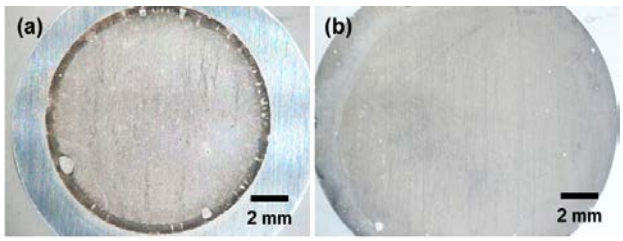

Fig. 2: Appearance of (a) as-polished and (b) HAp-coated Mg-0.2wt%Ca alloy immersed in the simulated body fluid for 1 day.

DISCUSSION & CONCLUSIONS: The surface micromorphology of HAp coatings formed on the Mg-Ca alloys was very similar to that formed on pure Mg [2]. It was revealed that small amount of Ca in alloys does not influence the micromorphology of HAp coatings. The corrosion area percentage was reduced and the corrosion morphology was changed with HAp coating.

REFERENCES: [1] S. Hiromoto et al. (2009) *Electrochim Acta* **54**: 7085-7093. [2] M. Tomozawa, S. Hiromoto (2011) *Acta Mater* **59**: 355-363. [3] S. Hiromoto, M. Tomozawa (2010) *Mater Trans JIM* **51**: 2080-2087. [4] S. Hiromoto et al. (in press) *J Mech Beh Biomed Mater*.

In vitro strategies to mimic *in vivo* events after osseous implantation

BJC Luthringer[1], L Wu[1; 2], M Costantino[1], A Burmester[1], AF Schilling[2], F Feyerabend[1], R Willumeit[1]

[1] *Department for Structural Research on Macromolecules, Institute of Materials Research, Helmholtz-Centre Geesthacht, Geesthacht, Germany*

[2] *Klinik und Poliklinik für Plastische Chirurgie und Handchirurgie, Technische Universität München, Munich, Germany*

INTRODUCTION: At least three important types of cells are interplaying before and after implantation of osseous medical devices: macrophages, osteoblasts, and osteoclasts. Even if the canonical cascade of events is understood, the effects of degradation products from magnesium-based implants on this scene remain unclear. To unveil these mechanisms, different *in vitro* models considering different aspects of interactions were developed. The successful implementation may decrease costs and avoid ethical issues of *in vivo* experiments while maximising experimental convenience.

METHODS: For osteoblasts, several cell lines (Saos-2, U2OS, and MG63) as well as primary cells (human bone derived cells (HBDC) and human umbilical cord perivascular (HUCPV)) were investigated. The U937 cell line (pro-monocytes) and peripheral blood mononuclear cells (PBMC) were selected as macrophage and osteoclast models, respectively[1]. The cell models were differentiated and the effect of magnesium ($MgCl_2$ and degradation products from magnesium implant material ("magnesium extract")[2]) on this process was investigated. Model-specific markers were followed by biochemical means (*e.g.*, real time PCR, Elisa tests, and microscopy).

RESULTS: The first issue was to find the most suitable cell model for the different stages of interaction. For osteoblasts only Saos-2 exhibit a similar protein and gene expression profile than primary cells, MG-63 the least comparable. Furthermore, a more drastic effect of magnesium extract than $MgCl_2$ on bone specific markers (*e.g.*, osteocalcin) was measured on HBDC supplemented with factors promoting osteogenic differentiation. For osteoclasts and macrophages, the attainableness of differentiated cells was another obstacle. To approbate the cell model, selection was performed on their ability to exhibit closed patterns to what has been reported *in vivo via i.e.*, specific osteoclast tartrate resistant acid phosphatase and cathepsin K or macrophage tumour necrosis alpha (TNFα) interleukin 6 & 1 alpha (IL6 & IL1β) activity /expression. Osteoclast (PBMC) and osteoclast / osteoblast models were successfully established and effect of magnesium on cell differentiation was observed[1]. While osteoclast activity was increasing with higher $MgCl_2$ concentrations, magnesium extract had a two-phase effect: first induced by low magnesium concentration and then reduced with higher concentrations. Similar results were obtained in co-culture model. Similarly, macrophages were obtained and characterised. The co-culture macrophage / osteoblast remains under set-up and the effect of magnesium is currently investigated.

DISCUSSION & CONCLUSIONS: More complex models were successfully established and characterised to investigate the intricate *in vivo* processes (inflammation / repair / remodelling) which are taking place during implantation. Magnesium extracts show in general different results as compared to Mg salt which is implying that other compounds/mechanisms are interplaying during *in vivo* magnesium-based implant degradation.

REFERENCES: [1] L. Wu, B. Luthringer, L. L. Grünherz, N.Wojtas, U. Hopfner, F. Feyerabend, R. Willumeit, A. F. Schilling (2013) Osteologie 2013, Weimar, Germany. [2] F. Feyerabend, H. Drücker, D. Laipple, C. Vogt, M. Stekker, N. Hort, R. Willumeit (2012) *J Mater Sci: Mater Med* **23**:9–24.

ACKNOWLEDGEMENTS: This research project has been supported by the Marie Curie Initial Training Network MagnIM (Grant agreement no.: 289163).

Influence of strontium concentration on *in vitro* corrosion property and cytocompatiblity of ternary Mg-Zn-Sr alloys

D Tie[1, 2], RG Guan[1], T Cui[1], LL Wu[2], LL Song[1], HM Qin[3]
[1] *Northeastern University, Shenyang, China.* [2] *HZG Research Center, Geesthacht, Germany.*
[3] *Northern Hospital, Shenyang, China.*

INTRODUCTION: Magnesium's functions in metabolic processes and its electrochemical reactivity make it ideal as degradable implants [1]. Mg-Zn-Sr alloys were proven suitable as potential biomaterials in our previous work [2]. In the present study, four Mg-Zn-Sr alloys designed by our own were compared to reveal Sr's influence on bio-corrosion process and cytocompatibility.

METHODS: ZJ41B (4.0wt% Zn, 0.5wt% Sr), ZJ41C (1.0wt% Sr), ZJ41D (1.5wt% Sr), ZJ42A (2.0wt% Sr) alloys and pure Mg were cast and rolled. Scanning electron microscopy (SEM) with energy dispersive X-ray spectroscopy (EDS) were employed for surface analysis. Immersion test in simulated body fluid (SBF) was carried out for 72h. The cytocompatibility of the alloys towards L929 cell line was characterized using polarizing microscope with fluorescent staining.

RESULTS: The size and amount of second phases increased with higher concentration of Sr (Fig. 1a).

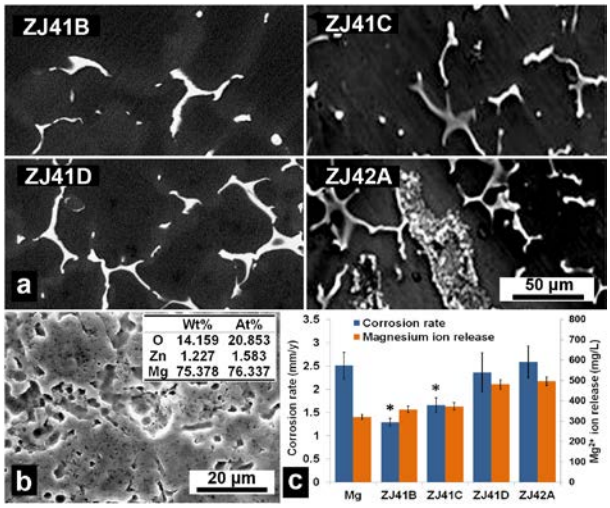

*Fig. 1: Microstructures of the four alloys (a); the SEM image and composition of corrosion layer by EDS area scanning of ZJ41B (b); corrosion rate calculated by mass loss and magnesium ion release (c). (Mean value ± SD, n=3, *p<0.05)*

Increasing general corrosion rate and ion release were observed as more Sr content presented, whilst ZJ41B (1.28±0.08mm/y) and ZJ41C (1.63±0.15mm/y) exhibited significantly lower corrosion rate than pure Mg (2.49±0.27mm/y, Fig. 1c).

After 72h cell culture, the survival rates of L929 cells on test alloys all exceeded 90% (Fig. 2). Higher concentration of Sr content did not induce additional cytotoxicity. Cell adhesion density and degree of cell extension was not significantly different from the control group (Fig. 2a).

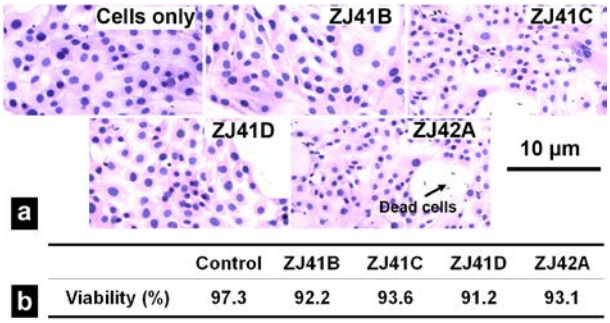

b

	Control	ZJ41B	ZJ41C	ZJ41D	ZJ42A
Viability (%)	97.3	92.2	93.6	91.2	93.1

Fig. 2: Polarizing microscope images of L929 cells on ZJ alloys after fluorescent staining (a); cell viability after 72h culture (b).

DISCUSSION & CONCLUSIONS: Presence of second phases improves the alloys' corrosion resistance by increasing general corrosion potential [3], which assures better cytocompatibility, while high concentration (>1.5wt%) of Sr accelerates the corrosion process by inducing localized corrosion. As an essential element for human body, Sr improves Mg alloys' corrosion and mechanical properties and also benefits bone generation [2, 4]. The alloys with 0.5-1.0wt% Sr content show the biggest potentials as biodegradable implant materials due to their balanced property profile.

REFERENCES: [1] F. Witte, et al (2008) *Curr Opin Solid St M* **12**:63-10. [2] F. Aaron, et al (2013) *J Mater Sci: Mater Med* **24**:989-15. [3] W. Zhou, et al (2010) *Corros Sci* **12**:1035-7. [4] P. Marie, et al (2001) *Calcif Tissue Int* **69**:121-9.

ACKNOWLEDGEMENTS: The authors are grateful to National Natural Science Foundation of China (Grant 51034002, 51222405 and 51074049).

In vitro studies on Mg-Ge(-Ca, Zn) alloy system newly-developed for potential biomedical applications

YF Zheng[1, 2], WR Zhou[2], L Ruan[3]

[1] *State Key Laboratory for Turbulence and Complex System and Department of Materials Science and Engineering, College of Engineering, Peking University, China.* [2] *Center for Biomedical Materials and Tissue Engineering, Academy for Advanced Interdisciplinary Studies, Peking University, China.* [3] *Department of Mechanical Systems Engineering, Graduate School of Science and Technology, Kumamoto University, Kurokami 2-39-1, Kumamoto-shi 860-8555, Japan*

INTRODUCTION: Germanium (Ge) is considered as biocompatible and from the viewpoint of material science, Ge can refine the grain size of magnesium alloys, improve the mechanical property as well as corrosion resistance. Therefore, Mg-Ge(-Ca, Zn) alloys are designed and fabricated in the present study and their potential biomedical application are studied.

METHODS: Five Mg-Ge(-Ca, Zn) alloys were melted and casted by pure element powers (Mg, Ge, Ca and Zn) under the protection of a mixed gas atmosphere of SF_6 and CO_2. Three kinds of the binary alloy ingots were further cut into 6 mm thick plates and hot rolled to about 2 mm thick sheets. Their microstructures were observed by X-ray diffraction and optical microscopy. Uniaxial tensile testing was conducted with an Instron 5969 universal testing machine at a crosshead speed of 1 mm/min. The biocorrosion properties were evaluated by electrochemical measurements and static immersion tests in Hank's solution. Furthermore, fibroblast L-929 and human osteoblast-like MG63 cell lines were cultured and responses between cells and different alloy extracts were assessed.

RESULTS: Mg-Ge(-Ca, Zn) alloys are composed of α-Mg and eutectic (α-Mg+Mg_2Ge). The tensile testing indicates higher strength and lower elongation of as-rolled Mg-Ge alloys compared to that of as-cast Mg-Ge alloys. Mg-2.5Ge and Mg-3Ge exhibit higher strength and elongation than Mg-1.5Ge. Ca reduces the strength and elongation of as-cast Mg-1.5Ge, while both of them are improved by the addition of Zn. Among these alloys, as-cast Mg-1.5Ge shows most rapid corrosion rate and severe corrosion morphology, and this is improved by hot-rolling and alloying with Ca and Zn elements. Mg-Ge(-Ca, Zn) alloys present non-toxicity for MG63 while a slight inhibiting effect is found for L-929 cell lines.

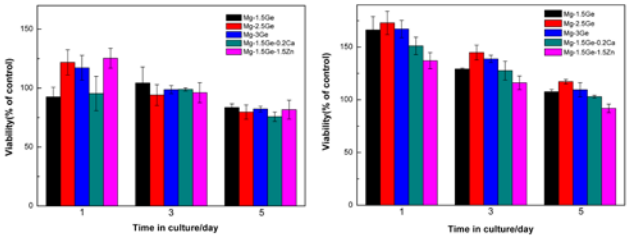

Fig. 1: Cell viability expressed as a percentage of the viability of cells cultured in negative control after 1-, 3- and 5-day incubations in the Mg-Ge(-Ca, Zn) alloy extracts: (a) L-929 and (b) MG63.

Table 1. Corrosion rates of Mg-Ge(-Ca, Zn) alloys calculated by electrochemical measurements and hydrogen evolution tests.

Alloy	V_{corr}(mm/y)	P_h (mm/y)
as-cast Mg-1.5Ge	4.32	5.06
as-cast Mg-2.5Ge	0.03	0.16
as-cast Mg-3Ge	0.02	0.22
as-cast Mg-1.5Ge-0.2Ca	0.16	0.37
as-cast Mg-1.5Ge-1.5Zn	1.55	0.76
as-rolled Mg-1.5Ge	0.82	1.25
as-rolled Mg-2.5Ge	0.31	0.58
as-rolled Mg-3Ge	0.02	0.13

V_{corr}, calculated by electrochemical measurements; P_h, calculated by hydrogen evolution tests.

DISCUSSION & CONCLUSIONS: Based on the results, Mg-Ge(-Ca, Zn) alloys show suitable mechanical properties, along with strong corrosion resistance and excellent biocompatibility *in vitro*, which means that it is of great potential to develop Mg-Ge(-Ca, Zn) alloys as a new kind of biodegradable material.

Corrosion of zinc in PBS, Ringer solution, blood plasma and whole blood

K Törne[1,2], AN Weissenrieder[2], J Weissenrieder[1]

[1]*Materials Physics, KTH Royal Institute of Technology, Kista, Sweden*
[2] *St Jude Medical Systems AB, Uppsala, Sweden*

INTRODUCTION: Zinc is a candidate metallic material for biodegradable implant applications[1,2]. Its corrosion rate in between magnesium and iron is suitable for several applications[1] and zinc exhibit favorable blood compatibility[2]. Here we investigate the corrosion mechanism of zinc in relevant electrolytes and evaluate plasma and whole blood as electrolytes for an improved *in vitro* model of corrosion.

METHODS: The electrochemical properties of pure zinc (>99.9%) in phosphate buffered saline (PBS), Ringer solution, plasma and citrated whole blood were investigated.

Initial corrosion rates were estimated from potentiodynamic polarization (PDP) analysis ±250 mV vs. open circuit potential.

Electrochemical impedance spectroscopy (EIS) analysis was performed on samples immersed in electrolyte for up to 72 h. The samples were investigated by scanning electron microscopy (SEM) and Fourier transform infrared spectroscopy (FTIR) both prior to and after immersion.

RESULTS: The initial corrosion rates as determined by PDP were, from lowest to highest, PBS < Ringer ~whole blood < plasma.

The Bode plots after 72h immersion are presented in Fig1. The polarization resistance at long immersion times increased in the order Ringer < PBS ~ whole blood < plasma. Both PBS and Ringer solutions exhibited spectra that have to be interpreted as a convolution of two time constants. The EIS results in PBS indicated localized corrosion and porous corrosion products on surface. This finding was also supported by the SEM analysis. The FTIR spectra of the surface exposed to PBS showed three distinct peaks (at 1640, 1000 and 950 cm^{-1}). In Ringer solution the formation of a gel-like layer was observed on the surface and the corresponding FTIR spectra had a series of peaks between 1540 and 700 cm^{-1}. In plasma and whole blood the EIS analysis showed equivalent circuit models alternating in immersion time between one and two time constants. The alterations in whole blood were marked by changes in the color of the electrolyte as well. SEM analysis revealed a homogenous layer of corrosion products.

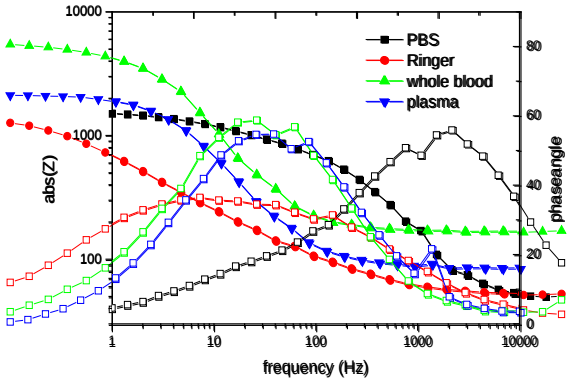

Fig. 1: EIS spectra from Zn samples exposed for 72 h in PBS (black), Ringer (red), plasma (blue), and whole blood (green)

DISCUSSION & CONCLUSIONS: The corrosion mechanism and the initial corrosion rate of zinc in PBS differ significantly from the other electrolytes in this study. FTIR identify phosphate as the main corrosion product. In Ringer solution zinc is characterised by formation of a uniform diffusion controlled layer. FTIR show the corrosion products as water containing carbonates. In plasma and whole blood the corrosion mechanism is characterised by the formation and detachment of organic layers (from FTIR). The initial corrosion rate is similar to in Ringer solution. Blood and plasma provide a good model for *in vitro* studies of initial corrosion (up to 24 h). For longer immersion times the stability of these electrolytes is a concern and Ringer solution is preferred. Improved cell design may increase the stability of whole blood and plasma.

REFERENCES: [1] Vojtech,D.; Kubasek, J.; Serak, J.; Novak, P., *Acta Biomaterialia* 2011, *7* (9), 3515-3522 [2] Cheng, J. et al., *J Mater. Sci. Technol. (2013), http://dx.doi.org/10.1016/j.jmst.2013.03.019*

ACKNOWLEDGEMENTS: The Swedish Research Council (VR) and St. Jude Medical AB are acknowledged for their financial support

Cytotoxicity evaluation of Mg-Sn-Mn alloy on mouse fibroblasts using iTRAQ-based quantitative proteomic analysis

L Yang[1], Z Zhen[1], C Lai[2,3], TF Xi[1,*]

[1]*Center for Biomedical Materials and Tissue Engineering, Academy for Advanced Interdisciplinary Studies, Peking University, Beijing, China.* [2]*Biomedical Research Center, Shenzhen Institution, Peking University, Beijing, China.* [3]*National Engineering Research Center for Biomaterials, Sichuan University, China.* [*]*Corresponding author*

INTRODUCTION: Magnesium-based materials are potential candidates for orthopaedic and cardiovascular biomaterials. In comparison with commercial magnesium-based alloys AZ31 and WE43, the recent development of Mg-3Sn-0.5Mn alloy revealed that it had better combined mechanical properties and corrosion resistance for the biodegradable stent materials [1]. However, there still has not been comprehensive biocompatibility evaluation of this alloy on living systems at the molecular level.

METHODS: To reveal molecular mechanisms of the interaction between magnesium and cells, isobaric tag for relative and absolute quantitation (iTRAQ)-coupled two dimensional liquid chromatography-tandem mass spectrometry (2D LC-MS/MS) approach and bioinformatics analysis were utilized to investigate the protein profile change of mouse fibroblasts L-929 cells treated by as-cast Mg-3Sn-0.5Mn alloy for 4, 8, 24, 48 h, respectively. WST-8 cell proliferation assay and flow cytometry experiment were used to evaluate the cellular response of L-929 cells to alloy.

RESULTS: A total of 909 unique proteins were identified by two or more peptides. Compared with the control cells, 121, 151, 135, 148 down-regulated proteins and 155, 81, 117, 113 up-regulated proteins were differentially expressed in Mg-3Sn-0.5Mn alloy-treated cells for 4, 8, 24 and 48 h, respectively. Many proteins showed altered expression in response to contact with Mg-3Sn-0.5Mn alloy at different time points.

Web Gene Ontology (WEGO) annotation [2] of the differentially expressed proteins showed that the L-929 cells which responded to Mg-3Sn-0.5Mn alloy covered a broad range of functional groups including cellular biological process, molecular function, and cellular component. Based on the molecular function categories, 75.9%-80.6% and 35.2%-38.9% proteins possessed the binding and catalytic activity, respectively. In the biological process category, most of proteins involved in metabolic process (61.8%-67.1%) and cellular process (76.6%-78.3%).

KEGG pathway analysis showed that Mg-3Sn-0.5Mn alloy treatment altered the metabolism, oxidative phosphorylation pathway, cytoskeleton, epithelial tight junctions and environmental information processing. Moreover, Mg-3Sn-0.5Mn alloy has extensive effects on L-929 cells by involving p53-dependant apoptosis and G1/S cell cycle arrest.

Cell proliferation test indicated that Mg-3Sn-0.5Mn alloy showed no negative effect on viability of L-929 cells. Flow cytometric analysis showed that Mg-3Sn-0.5Mn alloy treatment resulted in a slightly increase in the proportion of cells in the S phase compared with the control group. The proliferation index of cells in S phase showed a decline trend following time progression.

DISCUSSION & CONCLUSIONS: Through proteomic approaches, we found that Mg-3Sn-0.5Mn alloy could induce a cooperative response involving a wide panel of proteins and biological pathways. These result indicated that although the effect of Mg-3Sn-0.5Mn alloy to cells is not reflected at the cellular level, there has already been a significant change at the molecular level. It has been shown that iTRAQ-based quantitative proteomic analysis is an effective approach to clarify molecular mechanisms of cell-biomaterial interaction. The protein profile established in our study will be a great importance to evaluate biocompatibility of magnesium and its alloys.

REFERENCES: [1]X. Yang (2011) *Study on Microstructure and Properties of Biomedical Mg-Sn-Mn Alloy*, Harbin Engineering Univ. [2]J. Ye, L. Fang, et al (2006) *Nucleic Acids Res* 34: 293-7.

ACKNOWLEDGEMENTS: This work was supported by the National Basic Research Program of China (No.2012CB619102 and 2012CB933600).

Degradation and cytocompatibility of magnesium alloys for medical applications – an introduction to methods and observations

Huinan Liu[1,2]

[1]Department of Bioengineering, [2]Interdisciplinary Materials Science and Engineering Program, *Bourns College of Engineering, University of California, Riverside, CA. The United States*

INTRODUCTION: Magnesium (Mg) alloys are promising biodegradable metallic materials for orthopedic implants due to their many desirable properties. Mg has a mechanical strength and elastic modulus similar to cortical bone [1], and the degradation products can be naturally metabolized [2]. Furthermore, increased bone growth has been observed surrounding Mg derived implants *in vivo* [3]. However, rapid Mg degradation *in vivo* leads to rapid loss of mechanical properties of implants and acute increase of the local pH, thus limiting clinical translation of Mg alloys to orthopedic implants [4]. Significantly increased pH is often the primary reason for Mg cytotoxicity *in vitro* [5]. Many different experimental techniques have been used to investigate the cytocompatibility of Mg-based biomaterials and their *in vitro* interactions with cells, but the results of different experimental techniques are often not directly comparable to each other, even if the same research question is studied. The ability to compare experimental results among different literature reports is important to advance the field rapidly towards clinical translation. Therefore, this tutorial will first review and compare various *in vitro* techniques used to investigate cellular interactions with Mg-based biomaterials, and then emphasize the urgent need to establish standardized procedures for *in vitro* evaluation of Mg-based biomaterials.

DISCUSSION & CONCLUSIONS: One way to determine the cytocompatibility of Mg and its degradation products is to characterize the effects of Mg on cell proliferation *in vitro*. Both direct contact and indirect contact methods have been reported in literature to describe cell adhesion and proliferation in the presence of Mg alloys. For the direct contact method, cells are incubated directly upon the surface of Mg-based biomaterials. The direct method more closely represents the cell-implant interaction at the interface, which plays a critical role in implant success. Alternatively, for the indirect contact method, Mg-based samples are first degraded in water or buffer solutions since the amount of solubilized degradation products in the cell culture media depends on the degradation rate of Mg-based samples. Cells are then incubated with the soluble degradation products. In contrast to the direct contact method, the indirect contact method precisely controls the exact amounts of degradation products added into the cell culture media, and can allow the media pH values to be normalized across multiple groups. Some extent of standardization should not be difficult to implement in investigations. The combination of direct contact methods (such as PicoGreen or BrdU assay) and fluorescence microscopy to visualize cell adhesion and morphology may provide valuable, comparable information on cytocompatibility and cellular interactions with the biomaterial surface. Moreover, experimental conditions such as the type of cells used and cell-culture protocols (e.g. incubation time, type of media, frequency of media change, etc.) could be standardized to enable direct comparison of results in literature. Finally, consistent controls could provide benchmarks to compare cytocompatibility in different publications. Standardized cytocompatibility testing procedures can potentially enhance comparability of current literature reports on Mg-based biomaterials, promote worldwide data sharing, advance the field of biodegradable metals with more synergy, and accelerate clinical translation of Mg based biomaterials for biomedical implant and device applications.

REFERENCES: [1]H.S. Brar, M.O. Platt, M. Sarntinoranont, P.I. Martin, M.V. Manuel (2009) *JOM-US*, 61:31-34. [2]F. Witte (2010) *Acta Biomater*, 6:1680-1692. [3] C. Janning, E. Willbold, C. Vogt, et al. (2010) *Acta Biomater*, 6:1861-1868. [4]R.G. Guan, I. Johnson, T. Cui, et al. (2012) *J Biomed Mater Res A*, 100:999-1015. [5]C. Yang, G. Yuan, J. Zhang, Z. Tang, X. Zhang, K. Dai (2010) *Biomed Mater*, 5:045005.

ACKNOWLEDGEMENTS: The author appreciates financial support from Burroughs Wellcome Fund 2012 Collaborative Research Travel Grant, Hellman Faculty Fellowship, and the United States National Science Foundation (CBET 1125801).

Preincubation increases *in vitro* cell adhesion to magnesium and its alloys

F Feyerabend[1], A Möhring[2] and R Willumeit[1]

[1] *Helmholtz-Zentrum Geesthacht, Geesthacht, Germany* [2]*Christian-Albrechts-University Kiel, Kiel, Germany*

INTRODUCTION: Magnesium and its alloys are supposed to be promising materials for orthopedic applications. A general drawback is the applicability of common *in vitro* analyses like cell adhesion studies due to the degradation of the material by contact with aqueous solutions [1]. The reaction of the body to the implantation of foreign materials is time-dependent: As first step blood contact occurs, followed by an acute inflammatory response. Tissue cells get in contact with the material only at a later stage. Therefore the idea of this study was to simulate parts of this time flow by first incubating the materials in medium (simulating blood contact) and then adding the tissue cells after different periods of time.

METHODS: Pure Mg (99.99%) and the Mg10Gd1Nd alloy were extruded (Strangpreßzentrum Berlin, Germany) and afterwards machined to discs with a diameter of 10 mm and a height of 1.5 mm. Samples were sterilized with ethanol and used directly, or immersed in McCoy's medium with 10% fetal bovine serum for 0.5, 2, 6, 16, 24, 48 and 72 h prior to cell seeding. After this preincubation samples were transferred to agarose-coated 12 well plates to avoid unspecific cell adhesion. Saos-2 cells (ECACC, Salisbury, UK) were then applied (50.000 cells per sample in 50 µL medium). Afterwards the cells were incubated for 72 hours. Analyses were performed by Live/dead staining and SEM observations. Moreover, the alloying elements in the corrosion layer were analyzed by EDX and FT-IR.

RESULTS: Cell adhesion on the pure magnesium samples was generally lower than for the Mg10Gd1Nd alloy. Without pre-incubation, no living cells were observable on pure magnesium, whereas on the alloy already some cells were adherent. The amount of adhering cells could be greatly improved by the preincubation step, with an optimal range of >24 h for pure Mg and >6 h for the alloy (Fig.1)

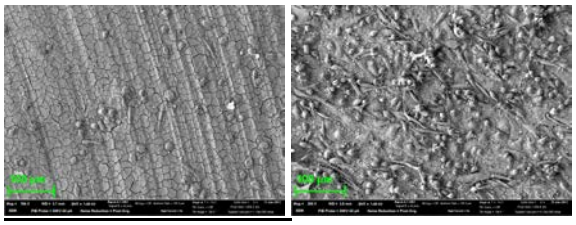

Figure 1: SEM-image of cell adhesion after 24 h preincubation. Left: pure Mg; right: Mg10Gd1Nd

The analysis of the corrosion layer by EDX indicated an accumulation of neodymium and a highly correlated distribution of Mg and gadolinium. However, this accumulation does not exhibit negative effects on the cells. FT-IR analysis revealed a distinct change of the sample surface over time. Initially observable brucite ($Mg(OH)_2$) disappeared, whereas the appearance of corrosion products containing N-H_x, O-H, C-C, C-O-O and C-O bonds was clearly observable.

DISCUSSION & CONCLUSIONS: By mimicking the order of events happening *in vivo*, a better cell adhesion could be obtained. This behavior is moreover correlated to the corrosion rate of the materials, as it was higher for the pure Mg than for the alloy (observed by measurement of pH and osmolality). By using the preincubation step in *in vitro* models a more realistic simulation of the *in vivo* environment may be achievable.

REFERENCES [1] Witte F, et al. Current Opinion in Solid State and Materials Science. 2008;12:63-72.

ACKNOWLEDGEMENTS: The authors want to thank Gabriele Salamon for expert technical assistance and Dr. Nico Scharnagl for assistance with the FT-IR measurements.